Microbial Ecology
https://doi.org/10.1007/s00248-022-01989-8

GENES AND GENOMES

Genomic Comparisons of Two *Armillaria* Species with Different Ecological Behaviors and Their Associated Soil Microbial Communities

Jorge R. Ibarra Caballero[1] · Bradley M. Lalande[1,2] · John W. Hanna[3] · Ned B. Klopfenstein[3] · Mee-Sook Kim[4] · Jane E. Stewart[1]

Received: 11 October 2021 / Accepted: 6 March 2022

Abstract

Armillaria species show considerable variation in ecological roles and virulence, from mycorrhizae and saprophytes to important root pathogens of trees and horticultural crops. We studied two *Armillaria* species that can be found in coniferous forests of northwestern USA and southwestern Canada. *Armillaria altimontana* not only is considered as a weak, opportunistic pathogen of coniferous trees, but it also appears to exhibit in situ biological control against *A. solidipes*, formerly North American *A. ostoyae*, which is considered a virulent pathogen of coniferous trees. Here, we describe their genome assemblies and present a functional annotation of the predicted genes and proteins for the two *Armillaria* species that exhibit contrasting ecological roles. In addition, the soil microbial communities were examined in association with the two *Armillaria* species within a 45-year-old plantation of western white pine (*Pinus monticola*) in northern Idaho, USA, where *A. altimontana* was associated with improved tree growth and survival, while *A. solidipes* was associated with reduced growth and survival. The results from this study reveal a high similarity between the genomes of the beneficial/non-pathogenic *A. altimontana* and pathogenic *A. solidipes*; however, many relatively small differences in gene content were identified that could contribute to differences in ecological lifestyles and interactions with woody hosts and soil microbial communities.

Keywords Armillaria root disease · Tree health · Genomes · Pathogenic · Beneficial fungi · Dysbiosis

Introduction

In recent decades, the genetics of fungal pathogenicity and symbioses have been studied in concert to identify potential patterns related to these divergent ecological roles. Genomic comparisons among pathogenic and symbiotic fungi have highlighted great diversity in gene content, genome size, repeat content, and number of chromosomes among fungi with distinct ecological roles (e.g., [1, 2]).

Within the Agaricales of basidiomycota, 13,000 species have been described and ecological roles and lifestyles among these range from saprophytes to pathogens to ectomycorrhizal symbionts [3]. Evolutionary studies suggest that ectomycorrhizal lifestyle likely arose from saprophytic fungi [4]. Historically, ectomycorrhizal (ECM) fungi were thought to have reduced numbers of genes encoding plant cell wall–degrading enzymes (PCWDEs), including carbohydrate degrading enzymes. Recent literature has suggested that ECM fungi contain diverse repertoires of these genes encoding PCWDEs [5]. ECM fungi typically retain the distinct suites of PCWDEs and carbohydrate-active enzymes

Jorge R. Ibarra Caballero and Bradley M. Lalande contributed equally to this work.

✉ Ned B. Klopfenstein
ned.klopfenstein@usda.gov

✉ Mee-Sook Kim
meesook.kim@usda.gov

✉ Jane E. Stewart
jane.stewart@colostate.edu

[1] Department of Agricultural Biology, Colorado State University, Fort Collins, CO 80523, USA

[2] Forest Health Protection, USDA Forest Service, Gunnison, CO 81230, USA

[3] Rocky Mountain Research Station, USDA Forest Service, Moscow, ID 83843, USA

[4] Pacific Northwest Research Station, USDA Forest Service, Corvallis, OR 97331, USA

Published online: 21 March 2022

(CAZymes) of their saprotrophic ancestors; some, like the fungal CAZymes acting on pectin (GH28, GH88, and CE8), are expressed in ECM fungi on ectomycorrhizal root tips [5]. Furthermore, little evidence suggests that common gene repertoires exist among ECM fungi [1]. The genome of *Laccaria bicolor*, a well-described ECM fungus, contained twice as many secreted CAZymes (glycoside-hydrolases (GH), polysaccharide lyases (PL), and carbohydrate esterases (C)) than polysaccharide biosynthetic and modifying enzymes [6]; however, this pattern was also observed in the forest root pathogen, *Heterobasidion annosum* [7, 8]. Similarly, both mutualistic and parasitic species of Agaricomycotina typically have an abundance of transposable elements [9]. Thus, differences in genomic content of Agaricales fungi with divergent ecological roles (e.g., saprophytes, pathogens, mycorrhizal symbionts, biological control agents) are difficult to detect.

The genus *Armillaria* (Basidiomycota, Agaricales) includes species that have diverse ecological roles within their respective environments. Several species are important plant pathogens of trees/woody plants, while several species are symbionts or even hosts of other organisms [10–12]. *Armillaria* species are also important decomposers in the forests where they occur, especially because they can degrade lignin [11]. Among *Armillaria* species, *A. solidipes* (formerly North American *A. ostoyae*) is considered one of the more virulent pathogens [13], although virulence varies depending on isolate, host age, and other factors [14]. *Armillaria mellea* and *A. borealis* are also considered virulent pathogens, while *A. gallica*, *A. cepistipes*, *A. gemina*, *A. calvescens*, *A. sinapina*, and *A. nabsnona* are considered less virulent or secondary pathogens [10, 12, 15, 16]. A recently described species, *A. altimontana*, formerly North American biological species (NABS) X, is also usually considered as a weak pathogen [17], but evidence for pathogenicity is not well documented [18].

Armillaria solidipes (as *A. ostoyae*) and *A. altimontana* have been documented to co-occur within forest stands in the inland northwestern USA [18–20]. A previous study in northern Idaho, USA, provided evidence that *A. altimontana* can provide natural biological control of Armillaria root disease of western white pine (*Pinus monticola*) caused by *A. solidipes*. In this study, *A. solidipes* was uncommon in areas dominated by *A. altimontana*, and trees colonized by *A. solidipes* were associated with a lower growth and survival than trees colonized only by *A. altimontana*. The results demonstrated that *A. solidipes* and *A. altimontana* have two different and contrasting lifestyles: *A. altimontana* was not harmful to western white pine within the northern Idaho planting site and further suggests that *A. altimontana* behaves as a long-term, in situ biological control agent against virulent *A. solidipes* [20]. However, little is known about site factors or differences in microbial communities that enabled *A. altimontana* to outcompete *A. solidipes* within specific areas of this site. Recognizing the genetic or underlying soil factors that drive host-fungal interactions may provide approaches for enhancing the management of Armillaria root disease.

The distribution, life cycle, pathogenicity, and evolutionary relationships have been studied for several *Armillaria* species [10, 12, 14, 16, 21–25]. Collins et al. [26] studied the genome and proteome of *A. mellea*, identifying carbohydrate-degrading enzymes, laccases, and lignin peroxidases among other gene-encoded proteins. Ross-Davis et al. [27] characterized the transcriptome of an *A. solidipes* mycelial fan infecting grand fir (*Abies grandis*), finding high expression of transcripts coding for PCWDEs, along with enzymes and ABC transporters that may help detoxify host-produced defense compounds. More recently, genomes of four *Armillaria* species (*A. cepistipes*, *A. gallica*, *A. ostoyae*, and *A. solidipes*) were sequenced by Sipos et al. [28]; this comparative genomic study revealed a rich repertoire of PCWDEs and pathogenicity-related genes in these *Armillaria* species regardless of their ecological lifestyles ranging from an aggressive pathogen to an exclusive decomposer. This study also identified expression of numerous pathogenicity-related transcripts and proteins during fruiting body and rhizomorph development [24, 28]. However, no studies have examined genomic differences between *A. altimontana* and *A. solidipes*, which may provide insights into genomic signatures of ecological lifestyles of fungi within Agaricales.

Assessing interactions among the soil fungi with different ecological lifestyles within the microbial communities is critical to understand disease development. As a well-known example, the association between mycorrhizal associations of fungi and roots allows for increased water and nutrient uptake that sustain tree health [29–33]. Microbes also breakdown litter and forest debris, which maintain forest health by improving soil quality and recycling nutrients that are required by plants [34–38]. In addition, pathogenic soil fungi function as selective agents that can cause mortality to maladapted trees, increasing the vigor and relative adaptation of residual trees in the stand [39–41]. In contrast, highly virulent soil pathogens can infect healthy tree roots, resulting in tree mortality that ultimately degrades the health of forest stands [41]. Additionally, the ability to favor beneficial microbes that inhibit root pathogens, which are notoriously difficult to mitigate, may enhance current management techniques [42, 43].

Soil metagenomics or metabarcoding can be used to identify important fungi, bacteria, and archaea associated with tree health [43]. Determinations of the soil microflora can allow evaluations of treatment (e.g., soil amendments, forest thinning, underburning) influences on naturally occurring microbial communities that favor or suppress forest root

diseases/pathogens, which could provide new approaches to manage Armillaria root disease [20, 44, 45].

Herein, we elucidate genomic and/or microbial soil profile differences associated with two *Armillaria* species that display divergent ecological lifestyles. We first present the genome assembly and annotation of the potentially beneficial *A. altimontana* isolated from northern Idaho, northwestern USA, and compare it with the genome of a pathogenic *A. solidipes* isolated from the same region. In addition, we compare the fungal and bacterial communities in the soil associated with the two *Armillaria* species. Putative secreted and non-secreted proteins encoded in each of the *Armillaria* genomes and the potential relationship with associated microbial communities are described, with emphasis on genes related to pathogenicity and fungal/ecological lifestyles. The data presented here contribute to understanding the ecological function of *Armillaria* species at the genomic level and will serve as resources for understanding genetic and ecological functions of these and other soil fungi.

Materials and Methods

Fungal Isolates for the Genome Sequencing

Armillaria solidipes (isolate ID001 [27]) was obtained from a culture of a basidiospore derived from a fruiting body belonging to a genet that was causing disease via an active mycelial fan growing below the bark of a live grand fir at the Clearwater National Forest, ID, USA. *Armillaria altimontana* (isolate 837–10) was obtained from a basidiospore from a fruiting body collected from the forest soil, with no host tree association ca. 2 km from the same location. After basidiospores were dispersed onto water agar, individual basidiospores were identified with a dissecting microscope and subcultured to establish haploid, basidiospore-derived cultures on 3% malt agar medium (3% malt extract, 3% dextrose, 1% peptone, 1.5% agar) for both species.

DNA Isolation

Isolates of *A. solidipes* and *A. altimontana* were grown for 3–4 weeks on 0.22-µm pore MF-Millipore™ Membrane nylon filters (MilliporeSigma, Burlington, MA) overlaying a membrane culture medium intended to reduce dark-colored exudates: 1.5% malt extract, 1.5% dextrose, 0.5% peptone, and 1.2% agar. The fresh mycelia (ca. 1–2 g) was scraped off from the nylon filter, ground by mortar and pestle with liquid nitrogen, and the DNA was extracted with the MoBio (Qiagen) DNeasy PowerMax Soil Kit (cat. no. 12988), following the protocol of the manufacturer.

Genome Sequencing and Assembly

PacBio sequencing and assembly of the two *Armillaria* species genomes were performed at the Laboratory for Biotechnology and Bioanalysis (LBB), Washington State University. Briefly, 10–15 µg of DNA were sheared using Covaris g-Tubes for 10 min at 1350 × g in a Minifuge 16 centrifuge (Beckman Coulter). Approximately, 5 µg of sheared DNA was processed for Pacific Biosciences SMRT bell library preparation following the "Procedure and Checklist-20 kb Template Preparation using BluePippin Size Selection System" (P/N 100–286-000–5) protocol (Pacific Biosciences) and the Pacific Biosciences SMRTbell Template Prep kit 1.0 (P/N 100–259-100). Resulting SMRTbell libraries were size selected using a BluePippin gel purification system (Sage Biosciences) according to the Blue Pippin User Manual and Quick Guide. The 0.75% agarose gel cassette was used with a cutoff limit set to 15–50 kb. The resulting SMRTbell library molecules had an average size of approximately ≥ 18 kb. Appropriate concentrations for the annealing and binding of the SMRTbell libraries were determined using the Pacific Biosciences Binding and Annealing calculator. SMRTbell libraries were annealed and bound to the P6 DNA polymerase for sequencing using the DNA/Polymerase Binding Kit P6 v2.0 (P/N100-372–700), following the recommended protocol from Pacific Biosciences but extending the binding times to 1–3 h, compared to suggested 30 min. The bound SMRTbell libraries were loaded onto the SMRT cells using the standard MagBead protocol and the MagBead Buffer Kit v2.0 (P/N 100–642-800). Then, the standard MagBead sequencing protocol was followed using the DNA Sequencing Kit 4.0 v2 (P/N 100–612-400) (typically known as P6/C4 chemistry). Sequencing data were collected for 6-h movie times, and Stage Start was enabled to capture the longest single reads possible. Genome assemblies were performed within the Pacific Biosciences SMRT Portal software. HGAPII was used following standard defaults for genome assembly.

Genome Assembly and Evaluation

Metrics for the genome assemblies, including scaffolds number, total length, GC content, and N50, were obtained using the QUAST [46] web server. Completeness of the assemblies was evaluated using BUSCO 2.0b2 [47]. BUSCO utilizes sets of genes present as single-copy orthologous in a number of species within a clade. For the evaluation of the *Armillaria* genome assemblies, the "Fungi dataset" and the "Basidiomycota dataset" were used. The default e-value of 0.001 was kept for the BLAST searches.

Phylogenetic Tree Analysis

Whole-genome phylogenetic tree was created using Realphy 1.12 [48] with Bowtie2 2.3.3.1 [49] for read mapping and PhyML [50] to build the tree. Preset options were used to run the Realphy pipeline. Whole-genome assemblies of *Armillaria* species available at the National Center for Biotechnology Information or the Join Genome Institute websites and the two genome assemblies described in this work were included. The number of bootstrap replicates in PhyML was set to 200.

Structural and Functional Genome Annotations

A set of repetitive sequences was obtained for each of the genome assemblies of *A. solidipes* and *A. altimontana* using RepeatModeler v.1.0.11 [51]. As the first step in the Maker v.2.31.8 pipeline [52], repetitive sequences files were used by RepeatMasker v.4.0.6 [53], to mask and obtain descriptions of interspersed repeats and low complexity DNA sequences. Next, the gene predictors Augustus [54], GeneMark-ES [55], and SNAP [56] were used for gene prediction in Maker. TRNAscan-SE [57] was also included to predict tRNA genes. For Augustus, a closely related species, *Coprinus cinereus*, was used as species model. SNAP was trained with a set of protein-encoding sequences from *Armillaria* species and closely related species, obtained from the NCBI and EnsemblFungi databases.

The set of proteins generated by Maker was functionally annotated using BLASTp v.2.9.0 + [58] and InterProScan v.5.20–59.0 [59]. Only proteins ≥ 50 amino acids were considered for these and further annotation analyses. For the BLAST search, a database was built with all entries for fungi in the UniProtKB database. A maximum e-value of 0.001 was used. For the InterProScan analysis, the Pfam application was included. Results from BLAST and InterProScan were added to the structural annotation in new gff3 files.

CAZymes were also annotated using the dbCAN2 server [60]; proteins involved in pathogenicity were searched using BLASTp at the PHI database version 46 [61]. Secondary metabolite clusters were annotated using antiSMASH server version 5.1.2 [62] with the detection strictness set to strict, including for the analyses the corresponding genome FASTA files of *A. altimontana* and *A. solidipes*. Deeploc 1.0, a program that utilizes deep learning algorithms [63], was used to predict the set of secreted proteins.

Structural Annotation Evaluations

Completeness of the *Armillaria* proteomes generated by Maker was evaluated using BUSCO 2.0b2. The "Fungi dataset" and the "Basidiomycota dataset" were used as assessed for the genome assemblies. The default e-value of 0.001 was also kept for the BLAST searches.

Synteny Analysis and Visualization

Analysis and graphs of synteny blocks (i.e., genomic regions of conserved gene content) were made using SyMAP 2.4 [64, 65]. Genome assemblies and GFF3 files produced by Maker were used to obtain the synteny graphs. Default parameters were used to run the program, except the minimum sequence size was set to 10,000 bp.

Analysis of Orthologous Protein Families

The set of predicted proteins generated by Maker for *A. altimontana* and *A. solidipes* were used to identify orthologous and species-exclusive (non-orthologous) groups using the OrthoVenn2 web server [66]. Two parameters can be adjusted when using the OrthoVenn2 web server: e-value and inflation value; they were set to 1e − 10 and 2, respectively. These values were chosen to slightly increase the detection of more non-orthologous proteins compared to the default values (1e − 2 and 1.5, respectively).

Study Area and Field Sampling for Soil Microbial Analysis

The study area was located in northern Idaho at the USDA Forest Service, Priest River Experimental Forest (Fig. 1). The field site was a historic western white pine seed provenance plot within the Ida Creek study area (ca. 48°21′48.75″ N and 116°49′25.36″ W, elevation ca. 770 m.a.s.l.). In 1971, 2372 seedlings from Idaho and Washington were planted in a common garden plantation [20]. In 1987, all 2076 remaining trees were sampled for diameter at breast height (DBH), height, tree health status, and association with *A. solidipes* and *A. altimontana*, as described by Warwell et al. [20].

In 2016, 60 trees were randomly selected for sampling, based on the historical plot distributions of *A. solidipes* and *A. altimontana*. Three additional trees (ca. 63) were sampled with needle discoloration and the formation of mycelial fans on the base of the trunk, indicating the presence of *A. solidipes*. Tree measurements included DBH and tree health status, which was based on total crown, foliage color, insect and disease presence, and dead/live status.

For soil sampling, 1 m from the main stem of a tree near root zones, depths of duff and litter were measured at each cardinal direction in a 30-cm-diameter circle. The area was then cleared, and bulk soil samples were taken for each of the 63 trees using a 15-cm, split soil corer with a 15.9-mm (5/8 inch), compact slide hammer (AMS, #400.99, American Falls, ID). Samples were homogenized, 2 g were placed

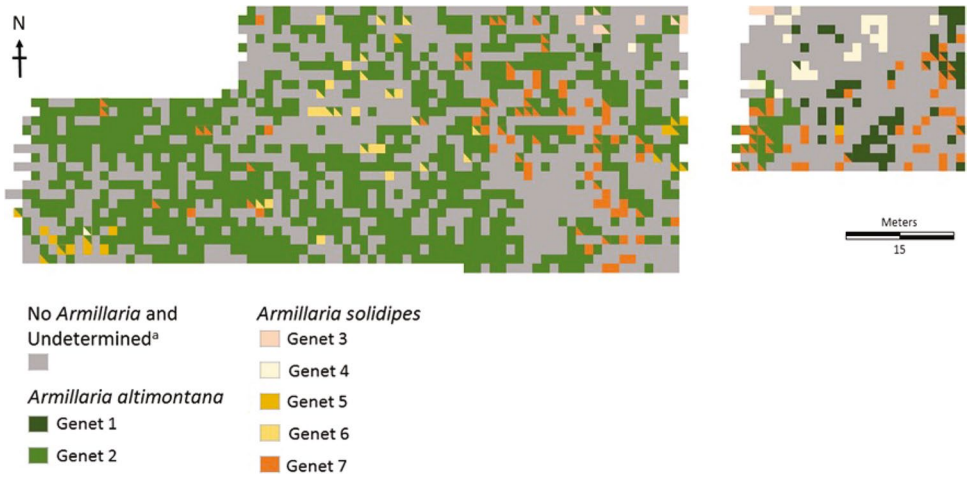

Fig. 1 Historical (1987) distribution of *Armillaria* species within the Ida Creek field site at the Priest River Experimental Forest, Idaho, USA. Pixels represent individual trees with colors representing the association between *Armillaria altimontana* or *A. solidipes*. Split pixels represent trees that were associated with both *A. altimontana* and *A. solidipes* (Warwell et al., 2019, 20)

in a 15-ml tube with 5 ml of LifeGuard RNA preservation solution (Qiagen®, Carlsbad, CA), and samples were placed on ice for preservation until storage. Samples were stored at − 80 °C prior to DNA extractions. Remaining bulk soils from each tree were sent to the USDA Forest Service, Rocky Mountain Research Station, Soils Laboratory in Moscow, ID, for soil characteristics measurements and chemistry calculations.

Armillaria rhizomorphs adjacent to the roots were also excavated using a small Pulaski-like gardening tool and brushes. Primary rhizomorph collections occurred on the same side as the soil core while an additional sample was collected 180° on the opposite side of the tree from the core. Rhizomorphs were placed in 15-ml tubes and placed on ice or 4 °C until isolation and culture.

Armillaria Isolation, DNA Extractions, and PCR

Rhizomorphs were plated for fungal isolation within 7 days of collection. Each rhizomorph was surface sterilized by an initial rinse with sterile-distilled water to remove the attached soil particles, followed by a soak in 20% Clorox® bleach solution (1.5% sodium hypochlorite, final concentration) for 6–10 min, a rinse with sterile-distilled water, and a soak in 3% hydrogen peroxide for 6–10 min. After a final rinse with sterile-distilled water, small rhizomorph sections (ca. 1-cm length) were plated onto 3% malt agar medium and incubated at 22 °C in the dark to promote mycelial growth of *Armillaria*.

For DNA extractions from *Armillaria* cultures, mycelia were sub-cultured onto Millipore™ membrane nylon filters that overlaid on membrane culture medium. After 2–3 weeks, mycelia were scraped off the nylon filters, and DNA was extracted from > 50 mg of mycelia using Zymo Fungal/Bacterial DNA extraction kits (Irvine, CA), following manufacturer protocols with a few modifications. To maximize DNA quantity and quality, three 3-mm glass beads were added to the cell lysis step prior to homogenization (Thermo Savant FastPrep ® FP120 Cell Homogenizer; Qbiogene, Carlsbad, CA) at 6.0 speed with two 30-s cycles. DNA concentration and quality were quantified using a NanoDrop™ 2000 spectrophotometer (Thermo Fisher Scientific, Wilmington, DE).

For species identification, DNA was amplified at the translation elongation factor-1α (*tef*1) locus using primers EF-983 and EF-2218 [67] with an Eppendorf Mastercycler pro Thermal Cycler (Eppendorf, Hamburg, Germany). The PCR cycle was 94 °C for 2.5 min, 30 cycles of 94 °C for 30 s, 60 °C for 30 s, and 72 °C for 1.5 min, with a final cycle at 72 °C for 10 min. PCR products were visualized using gel electrophoresis, cleaned with ExoSAP-IT™ PCR Product Cleanup Reagent (Thermo Fisher Scientific, Santa Clara, CA), and then Sanger sequenced in two directions by Eurofins Genomics (Louisville, KY). Sequences were edited and aligned in Geneious R11.1 (https://www.geneious.com). Aligned sequences were identified by comparing to the NCBI (National Center for Biotechnology Information) database using BLASTn (https://blast.ncbi.nlm.nih.gov/Blast.cgi) [58].

Soil DNA Extraction Protocol and Sequencing

DNA was extracted from the soil samples preserved in LifeGuard™ Preservation Solution using MoBio Powersoil Total RNA Isolation and DNA Elution Accessory kits (Qiagen®, Carlsbad, CA), following manufacturer protocols. DNA qualification and quality were measured using a Nanodrop™ 2000 spectrophotometer.

Soil DNA (30 µl) was sent to the University of Minnesota Genomics Center and Colorado State University Next-Generation Sequence (NGS) lab for library preparation and sequencing on an Illumina MiSeq and paired-end 2 × 250 reads were generated. Out of 63 samples, a total of 57 were sent for sequencing; the six remaining samples were

excluded because they did not yield sufficient DNA concentration/quality. Libraries were prepared for the internal transcribed spacer (ITS2) region to sequence fungal communities and the v4 genomic region of the 16S rRNA to sequence bacterial communities. Primers ITS3 (5′-GCATCGATG AAGAACGAGC-3′) and ITS4 (5′-TCCTCCGCTTATTGA TATGC-3′) [68] were used to amplify the ITS2 region, and primers 515F (5′-GTGCCAGCMGCCGCGGTAA-3′) and 806R (5′-GGACTACHVHHHTWTCTAAT-3′) [69] were used to amplify the v4 region of the 16S rRNA. DNA-free samples were included as negative controls to verify lack of microbial or DNA contamination in the buffers and primer sets. These sequence data have been submitted to the NCBI SRA database under accession number PRJNA767898.

Cleaning DNA Sequence Data

Data were cleaned to ensure base-calling accuracy of ≥ 99.9% using the paired-end mode in the program Trimmomatic v0.36 [70]. Sequences ≤ 100 bp in length, low-quality bases scores (≤ 15), and 4 bp sliding window regions with low average-quality scores (≤ 25) were removed from the data set. The software Mothur v1.40.5 [71] was implemented utilizing the standard operating procedure [72], with some adjustments, to call operational taxonomic units (OTUs) and classification of taxa. Following adjustments described in the SOP (https://github.com/Abdo-Lab/Microbiome-Analysis-Scripts/blob/master/PE-de-novo-processing.pl), UCHIME [73] was used for de novo identifications and removal of de novo chimeric sequences, and USEARCH [74], utilizing the dgc (distance-based greedy clustering) option, was used for clustering. Groups that were ≥ 97% similar were classified as belonging to the same OTU. Sequences associated with lineages of chloroplast, mitochondria, archaea, and bacteria were removed from the table of classified sequences. We utilized the 128 Silva database [75] and the UNITEv6_sh_dynamic_s [76] databases for bacterial and fungal taxonomic classifications, respectively, using Wang's Naïve Bayes classifier with a cutoff value of 80 [77]. Rarefaction curves were generated using the package "vegan" as implemented in R version 3.6.1 to assess diversity and suitability of depth of coverage per sample [78].

Statistical Analysis of Soil Microbial Communities

Using the RStudio interface to R (R Core Team 2017), alpha diversity, including Shannon diversity index and Inverse Simpson, was calculated using phyloseq [79], and rarefied richness (Richness) was determined in Vegan. Shannon's index was used to determine diversity utilizing the relationship to richness and rare microbes [80, 81]. Inverse Simpson was used to identify diversity based on evenness and more dominant microbes [81]. Richness was considered as the number of individuals identified within a single sample, while evenness was used to explain the relative abundance of the different individuals [82].

The relative abundance of taxa associated with *A. solidipes*- and *A. altimontana*–associated soils was determined for the top fungal and bacteria taxa using a stacked bar graph with the metagenomeSeq package in R [83]. Differences among communities associated with *Armillaria* species were assessed using a PERMANOVA. Principle component analysis plots were completed in vegan to visualize fungal and bacterial soil differences associated with each *Armillaria* species.

Utilizing relative abundance data based on the resulting OTU table, bar graphs were generated using the ggplot2 package [84] in R for observed taxa with relative abundance > 1% at the genus level to describe the microbial community structure associated with each *Armillaria* species. The metagenomeSeq package [83] in R was used to fit a model that identified those OTUs associated with significance of model fit at a 0.01 level and minimum fold change of 2 (*p* values were adjusted for multiple testing), which was used to identify the driver of OTU differences between treatments. Core fungal and bacterial communities were created for each *Armillaria* species. Counts were calculated in R to assess the presence of an OTU corresponding to each species of *Armillaria*. Venn diagrams were produced using molbiotools.com to identify unique and shared fungal and bacterial taxa associated with *A. solidipes* and *A. altimontana*.

To identify influences of soil chemistry properties on soil fungal communities, a PERMANOVA analysis was completed using the vegan package in R. The analysis identified significant predictors by completing a forward stepwise analysis based on the subset of variables that minimized the Akaike information criterion (AIC).

Results

Genome Assemblies of *A. solidipes* and *A. altimontana*

The PacBio assemblies resulted in a 73,739,702-bp genome for *A. altimontana* isolate 837–10 and a 55,735,298-bp genome for *A. solidipes* isolate ID001; both isolates originated near Elk River, ID, USA (Table 1). The ratio of genome sizes, *A. altimontana*/*A. solidipes* = 1.32, is consistent with the ratio of the reported DNA content per nucleus of these two species, 1.34 [19]. The corresponding genome assemblies were deposited at the NCBI with accession numbers JAIWYR000000000 for *A. altimontana* and JAIWYQ000000000 for *A. solidipes*.

In a whole-genome phylogenetic tree, two *A. solidipes* isolates from North America, ID001and 28–4, group

Table 1 Genome assembly metrics for *Armillaria altimontana* and *A. solidipes*

Feature	*A. altimontana*	*A. solidipes*
No. of scaffolds	100	72
Total length	73,739,702	55,735,298
Largest contig	5,843,527	4,463,803
GC (%)	47.77	48.26
N50	1,930,169	2,424,439

together (Fig. 2), apart from but close to isolate C18/9 of *A. ostoyae* from Europe [28]. Figure 2 also shows the position of *A. altimontana* with respect to *A. solidipes* and other *Armillaria* species. *Armillaria altimontana* is contained within a clade comprising *A. cepistipes* B5 and *A. gallica* Ar21-2, which is distinct from the *A. solidipes/ostoyae* clade.

After a custom library of repeats obtained using RepeatModeler was input to RepeatMasker, more bases in *A. altimontana* (18,346,415 bp) were masked compared to those in *A. solidipes* (9,691,790 bp). When comparing *A. altimontana* to *A. solidipes*, the relative proportion of masked bases (1.89) was larger than the ratio of their genome sizes (1.32). The percentage of genomic sequences occupied by interspersed repeats and low complexity DNA regions for *A. altimontana* and *A. solidipes* were 24.88% and 17.39%, respectively (Table S1); the largest percentages corresponded to retrotransposons. The most abundant retrotransposons were long terminal repeats (LTRs) as is common in other fungi [85].

Completeness of the genome assemblies was assessed using BUSCO using datasets for both the fungal and basidiomycota lineages. The *A. altimontana* genome assembly was 95.1% complete when compared to the fungal dataset and 96.7% when compared to the Basidiomycota dataset. The completeness values for *A. solidipes* were similar at 95.9% and 96%, respectively, and similar to those reported for other *Armillaria* species [28], which indicates high quality for genome assemblies.

Large blocks of shared synteny were found when comparing the *A. altimontana* and *A. solidipes* genomes (Fig. 3A shows the 20 largest scaffolds of each species), especially for some of the largest scaffolds of each species (Fig. 3B–G). For example, most of *A. altimontana* scaffold 1 (5,843,527 bp) shared synteny with blocks in two *A. solidipes* scaffolds (1 and 2; Fig. 3B), most of *A. altimontana* scaffold 2 (5,540,602 bp) shared synteny with blocks in three *A. solidipes* scaffolds (10, 14, and 18; Fig. 3C), and most of *A. altimontana* scaffold 3 (4,489,203 bp) shared synteny with blocks in two *A. solidipes* scaffolds (7 and 11; Fig. 3D).

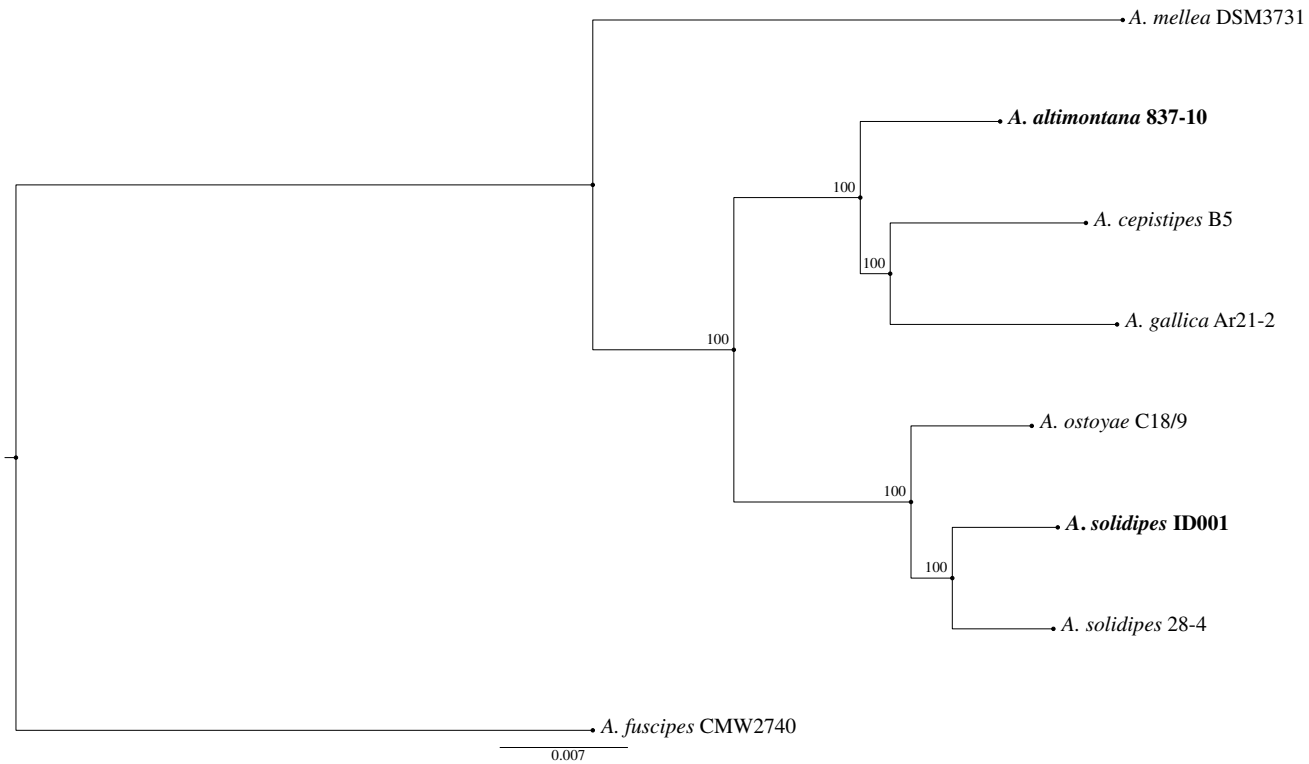

Fig. 2 Whole-genome phylogenetic tree of *Armillaria* species: *Armillaria mellea* DSM3731 (France), *A. altimontana* 837–10 (Idaho), *A. cepistipes* B5 (Italy), *A. gallic*a Ar21-2 (Vermont), *A ostoyae* C18/9 (Switzerland), *A. solidipes* ID001 (Idaho), and *A. solidipes* 28–4 (Vermont)

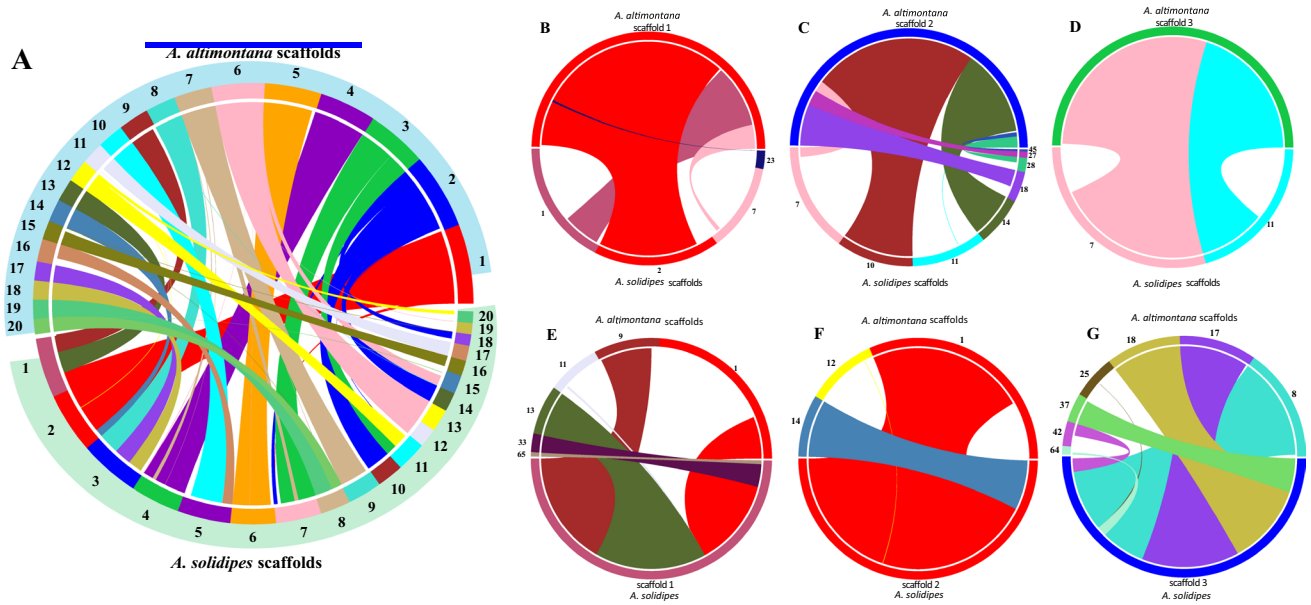

Fig. 3 Blocks of synteny comparing the 20 largest scaffolds of each *Armillaria* species (**A**); **B**–**D** block of synteny of the three largest *A. altimontana* scaffolds with *A. solidipes* scaffolds; **E**–**G** blocks of synteny of the three largest *A. solidipes* scaffolds with *A. altimontana* scaffolds

Likewise, most of *A. solidipes* scaffold 1 (4,463,803 bp) shared synteny with blocks in three *A. altimontana* scaffolds (1, 9, and 13; Fig. 3E); most of *A. solidipes* scaffold 2 (4,456,508 bp) shared synteny with blocks in two *A. altimontana* scaffolds (1 and 14; Fig. 3F); and most of *A. solidipes* scaffold 3 (4,392,256 bp) shared synteny with blocks in four *A. altimontana* scaffolds (8, 17, 18, and 37; Fig. 3G). A number of other smaller complete scaffolds of each species also shared synteny with blocks in one or more scaffolds of the other species (Fig. 3A).

Structural and Functional Annotation

The Maker annotation pipeline predicted several features for the genome assemblies, including CDs, exons, 5′-UTRs, genes, mRNAs, 3′-UTRs, and tRNAs, which were organized in GFF3 files (Table 2; Supplementary Files 1 and 2). High similarity was observed between the genomes of *A. altimontana* and *A. solidipes*. More protein-coding genes were present in the *A. altimontana* genome (19,130 versus 16,105), although the ratio of protein-coding genes, 1.18, is a little smaller than the ratio of genomes sizes (1.32). Despite its smaller genome, the *A. solidipes* genome contained more tRNAs genes (315 versus 280) (Table 2).

Completeness of the predicted proteomes was assessed using BUSCO, again with datasets for both the fungal and Basidiomycota lineages. For *A. altimontana,* proteome completeness was 96.9% when compared to the fungal dataset and 96.4% when compared to the Basidiomycota dataset. Proteome completeness values for *A. solidipes* were 97.2% and 96.7%, respectively, indicating high quality of the genome structural annotations.

Table 2 Genome features of *Armillaria altimontana* and *A. solidipes*

Feature	*A. altimontana*	*A. solidipes*
Genes	19,326	16,357
Average gene length (bp)	1504	1563
Gene density (genes per Mb)	262	293
Average exons per gene	5.2	5.6
Average exon length (bp)	219.8	217.2
Average introns per gene	4.2	4.6
Average intron length (bp)	85.9	75.3
tRNA genes	280	315
transcripts/proteins[a]	19,130	16,105

[a]Some genes are predicted to code for more than one protein

Predicted proteins sets for *A. altimontana* and *A. solidipes* (Supplementary Files 3 and 4) were functionally annotated using BLASTp against all the fungi entries in the Uniprot database and by using InterProScan including the Pfam application. These results were added to the final genome models produced by Maker, in GFF3 format (Supplementary Files 1 and 2). For *A. altimontana*, 17,997 encoded proteins had a BLASTp hit, and 8483 had an InterProScan (Pfam) hit (94.0% and 44.3% of the total, respectively). For *A. solidipes*, 15,449 encoded proteins had a BLASTp hit, and 8132 had an InterProScan (Pfam) hit (95.9% and 50.4% of the total, respectively).

In comparisons with other *Armillaria* proteomes, 9061 *A. altimontana* isolate-encoded proteins had a BLASTp hit to *A. gallica* proteins, 4723 to *A. ostoyae* proteins, and 3906 to *A. solidipes* proteins (8629 to *A. ostoyae/solidipes* proteins) (Supplementary Files 3 and 4). For our *A. solidipes* isolate–encoded proteins, only 1321 had a BLASTp hit to *A. gallica* proteins, 6665 to *A. ostoyae* proteins, and 7300 to other *A. solidipes* proteins (13,795 to *A. ostoyae/solidipes* proteins).

Secreted Proteins The program Deeploc was used to obtain corresponding sets of putative secreted proteins of *A. altimontana* and *A. solidipes* to search for differences that might reflect their lifestyle differences. A total of 1235 (6.4% of the total) secreted proteins were predicted in *A. altimontana*, and 1157 (7.1%) were predicted in *A. solidipes*. In *A. altimontana*, 322 secreted proteins had a CAZyme annotation, and 2 were cytochrome P450; in *A. solidipes*, the number of hits in each category was similar: 316 as CAZYmes, and 3 were cytochrome P450. No secreted proteins from either species had a blast hit with identity above 95% to proteins in the PHI database (data not shown). Some of the proteins had a CAZyme and a BLASTp hit, with one or several hits in the InterProScan search. But 99 secreted proteins in *A. altimontana* produced no hits and another 436 produced only BLASTp hits to uncharacterized proteins; in *A. solidipes*, 69 secreted proteins produced no hits and another 421 produced only BLASTp hits to uncharacterized proteins. However, many of these uncharacterized proteins could be considered "small secreted proteins" (see below). All those different annotations were combined and manually curated (Supplemental Files 3 and 4).

Numbers of secreted proteins with putative involvement in pathogenicity were obtained for each *Armillaria* species. The differences between the two species were small (Fig. S1); the two major differences were a higher number of peptidases secreted by *A. solidipes* and a higher number of small secreted proteins for *A. altimontana*.

When grouped by probable function (Fig. 4), the major differences in predicted secreted proteins of *A. altimontana* and *A. solidipes* were associated with cell wall–degrading enzymes. *Armillaria solidipes* showed a slightly larger number of enzymes that degrade plant cell wall components: cellulose, hemicellulose, lignin, and especially pectin. Encoded protein-degrading enzymes also were more abundant in *A. solidipes* compared to *A. altimontana* (Fig. 4). Abundances of other encoded protein categories showed smaller differences.

The number of encoded proteins that could be considered "small secreted proteins," defined as those smaller than 300 amino acids (after being predicted as "extracellular"), was 678 (~55% of total secreted) in *A. altimontana*, 381 with ≥2% cysteine residues, and 594 (~51% of total secreted) in *A. solidipes*, 334 with ≥2% cysteine residues. Numerous encoded small secreted proteins (205 in *A. altimontana* and 172 in *A. solidipes*) were annotated as

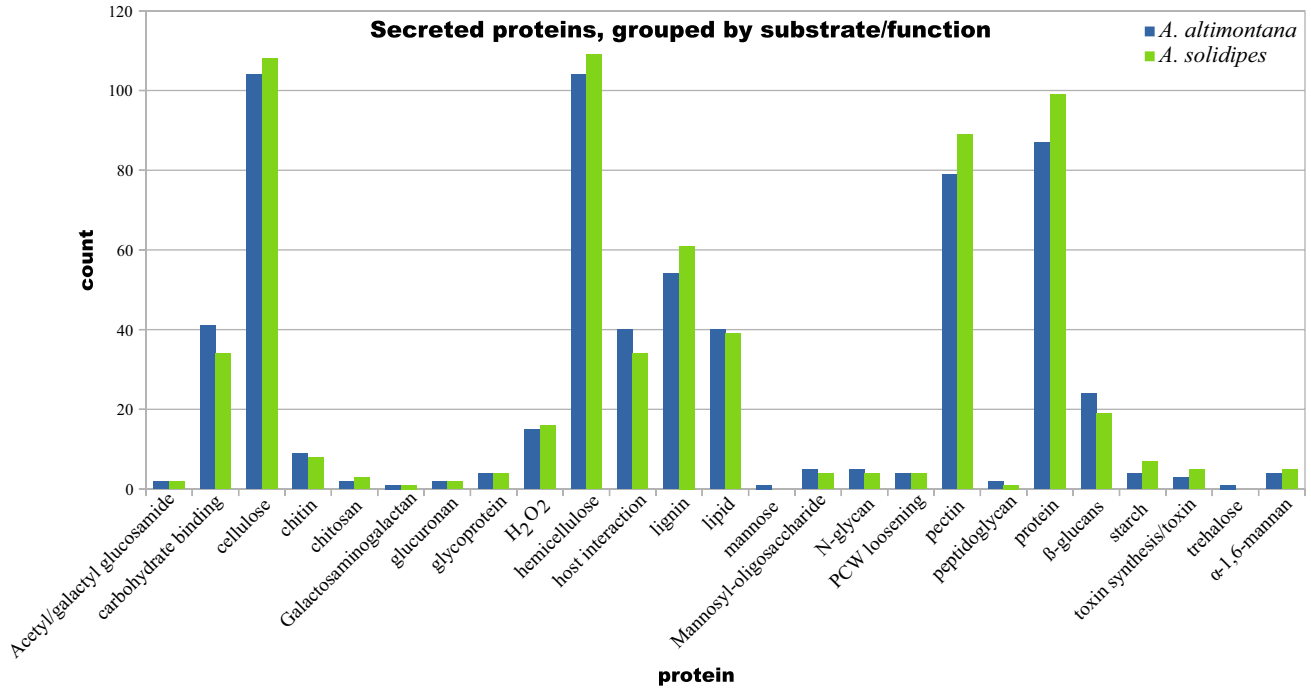

Fig. 4 Comparison of the number of pathogenicity-related secreted proteins in *Armillaria altimontana* and *A. solidipes*, grouped by function. Small secreted proteins are not included. All CBM genes were considered with a "carbohydrate binding" function

CAZymes, peptidases, thaumatin, cerato-platanin, hydrophobins, etc. (Supplemental Files 3 and 4); however, for other predicted small secreted proteins (375 in *A. altimontana* and 353 in *A. solidipes*), the only annotation were BLASTp hits to "uncharacterized protein," and there was no annotation for other predicted proteins (98 in *A. altimontana* and 69 in *A. solidipes*).

Non-secreted Proteins Numerous different functions were found among encoded proteins considered as non-secreted. Among them, those that matched CAZymes, cytochrome P450, transporters, or secondary metabolite clusters were further examined (Table 3). Transporters and secondary metabolites clusters were also included in these analyses because they have also been considered important for the lifestyle of fungal species [86, 87]. The abundance of encoded proteins annotated as CAZymes, ABC transporters, and secondary metabolite clusters was similar between *A. altimontana* and *A. solidipes* (Table 3), whereas numbers of cytochrome P450 and all transporters were larger in *A. altimontana*. However, the ratio *A. altimontana*/*A. solidipes* encoded protein numbers for most categories was smaller than the ratio of the genome sizes (1.32) and total proteins (1.18); only cytochrome P450 ratio was slightly higher (1.25) than the ratio of total proteins (Table 3).

When the abundance of the non-secreted CAZymes was grouped by substrate, the largest differences were found within encoded pectin-degrading enzymes with 58 in *A. altimontana* and 47 in *A. solidipes*; carbohydrate binding with 17 and 8, respectively; and lignin-degrading enzymes with 49 and 41, respectively (Fig. S2). Overall, most non-secreted CAZyme numbers were typically higher in *A. altimontana* in comparison with *A. solidipes*.

Table 3 Total number of non-secreted proteins by gene family for *Armillaria altimontana* and *A. solidipes*. The genome sizes were included for comparison

Feature	*A. altimontana*	*A. solidipes*	Ratio
Total non-secreted	17,895	14,948	1.19
CAZymes-cytochrome P450	334–242	305–195	1.09–1.25
Total transporters	474	414	1.14
ABC transporters	67	60	1.11
Secondary metabolite clusters	21	19	1.10
Total proteins	19,130	16,105	1.18
Genome size	73,739,702	55,735,298	1.32

Genes Upregulated in Rhizomorphs

We searched for genes reported by Sipos et al. [28] as notable genes that were upregulated in rhizomorphs. Most of the categories had similar numbers between both *Armillaria* species, although *A. altimontana* possessed 62 more genes encoding cytochrome P450 (Table 4). A diversity of functions has been ascribed to cytochrome P450 proteins [88–91]. Caspase domain–containing proteins, part of proteases that have been associated with programed cell death in other organisms [92], were more abundant (10 more) in *A. solidipes* (Table 4). Relatively large differences were also found in numbers of genes encoding two enzymes involved in secondary metabolites synthesis: polyprenyl synthase, involved in terpenoid synthesis [93, 94]: *A. altimontana* had 23 and *A. solidipes* had 12. In contrast, genes encoding trichodiene synthase, which utilize terpenoids to produce the trichodiene [94], were more abundant in *A. solidipes* with 12, compared to *A. altimontana* with only had three (Table 4).

Orthologous and Non-orthologous Proteins

Although approximately 62% of *A. altimontana* and 72% of *A. solidipes* predicted proteins grouped in 10,989 clusters of orthologous proteins, a large number, 7232, of proteins were non-orthologous in *A. altimontana*, and 4575 were non-orthologous in *A. solidipes* (Fig. 5A).

Out of the 10,989 clusters of orthologous proteins, 10,321 were two-protein clusters, which composed of one protein from each species; only 29 clusters had a difference larger than five proteins (Table 5). Of those, *A. altimontana* had more proteins in 24 clusters, whereas *A. solidipes* had more proteins in five clusters. Out of those 29 clusters, one cluster contained CBM67 proteins, which bind rhamnose residues in pectin, with 15 proteins from *A. altimontana* versus only one from *A. solidipes*. Another cluster contained ABC transporters, of which, *A. altimontana* also had 10 more than *A. solidipes*. Two clusters contained caspase domain proteins, with 17 more from *A. solidipes* than from *A. altimontana*. Other clusters corresponded to transposases, transcription factors, helicases, F-box proteins, and histone-modifying enzymes, while no annotation was found for 14 clusters (Table 5).

CAZymes and cytochrome P450 enzymes were found among non-orthologous proteins (Table 5). The number of non-orthologous CAZymes was 91 in *A. altimontana* and 80 in *A. solidipes*, with small differences in number of individual CAZymes between the two species, which are similar to the differences found in secreted and non-secreted CAZymes. A few non-orthologous CAZymes were exclusive, but only GT32 was found exclusively in *A. altimontana* among CAZymes with a count > 5. For cytochrome P450,

Table 4 Number of notable genes with overexpression in rhizomorphs (Sipos et al. 2017; 27) in the *Armillaria altimontana* and *A. solidipes* genome assemblies

Protein coded (Pfam terms)	*A. altimontana*	*A. solidipes*
Expansin (PF03330)	12	8
Bzip transcription factor (PF00170)	5	5
Zinc finger c2h2 (PF00096, PF12874, PF12756, PF06220, PF16278, PF08790)	62	68
Caspase domain (PF00656, PF14538)	30	40
Hydrophobin (PF01185)	7	4
Cytochrome P450 (PF00067)	271	209
GH28 (PF00295)	17	16
Pectinesterase (PF01095)	9	10
GH88 (GH105) (PF07470)	6	5
PL3 (PF03211)	9	10
GH3 (PF00933)	16	14
GH43 (PF04616)	11	10
GH76 (PF03663)	6	5
AA9 (PF03443)	18	21
Total cellulases	183	179
Cellulase (PF00150)	19	19
POD (PF00141; PF11895)	10	11
HTP (PF01328)	6	6
Laccase (PF00394)	25	28
Cerato-platanin (PF07249)	4	4
Carboxylesterase (PF00135)	32	37
Family 6 bacterial extracellular solute–binding protein (PF13343)	2	1
Polyketide synthase (PF14765)	10	7
Trichodiene synthase (PF06330)	3	12
Polyprenyl synthase (PF00348)	23	12

the difference was larger, with 39 more in *A. altimontana* (Table 5), and slightly smaller than the difference, 47, of total cytochrome P450 proteins (242 in *A. altimontana* vs 195 in *A. solidipes*; Table 3).

Many other proteins that were present in both *A. altimontana* and *A. solidipes* with the same Pfam-Interpro annotation were still considered non-orthologous by OrthoVenn2, and their numbers were also similar in most cases. Those with a number difference > 5 included polyprenyl synthase, trichodiene synthase, F-box protein, and glutathione S-transferase (Table 5). Other proteins were present only in one *Armillaria* species; most of these occurred in small numbers: three with counts > 5: Clp amino terminal domain pathogenicity island component; DDE superfamily endonuclease, only in *A. altimontana*; and sodium/hydrogen exchanger family, only in *A. solidipes*. Other non-orthologous proteins with smaller numbers, but with a possible functions in host–pathogen interactions, included terpene synthase (4) and transcriptional activator of glycolytic enzymes (4), which were found only in *A. altimontana* (Table 5).

Finally, 344 *A. altimontana* non-orthologous proteins were predicted as secreted with 327 of these representing small secreted proteins. For non-orthologous proteins from *A. solidipes*, 265 were predicted as secreted with 248 of these representing small secreted protein (Table 5).

Armillaria Species Identified from Field Plots

Rhizomorphs were isolated from 51 total trees, yielding 87 rhizomorph samples that all produced pure *Armillaria* cultures. Based on *tef1* sequencing of the 87 cultures from rhizomorph samples, 48 trees were associated with *A. altimontana*, and three trees were associated with *A. solidipes*. Rhizomorph isolation was unsuccessful for 12; therefore, these samples were not utilized in analyses. Sequences corresponding to both *A. altimontana* and *A. solidipes* resulted in 99% identity during BLAST searches on the NCBI database.

Processing Sequenced 16S and ITS2 Libraries in Mothur

From the soil samples, a total of 2,156,476 and 4,323,028 raw paired-end 2 × 250 bp reads from 56 samples were generated from 16S and ITS sequencing, respectively. For the 16S dataset, the mean sequencing depth after

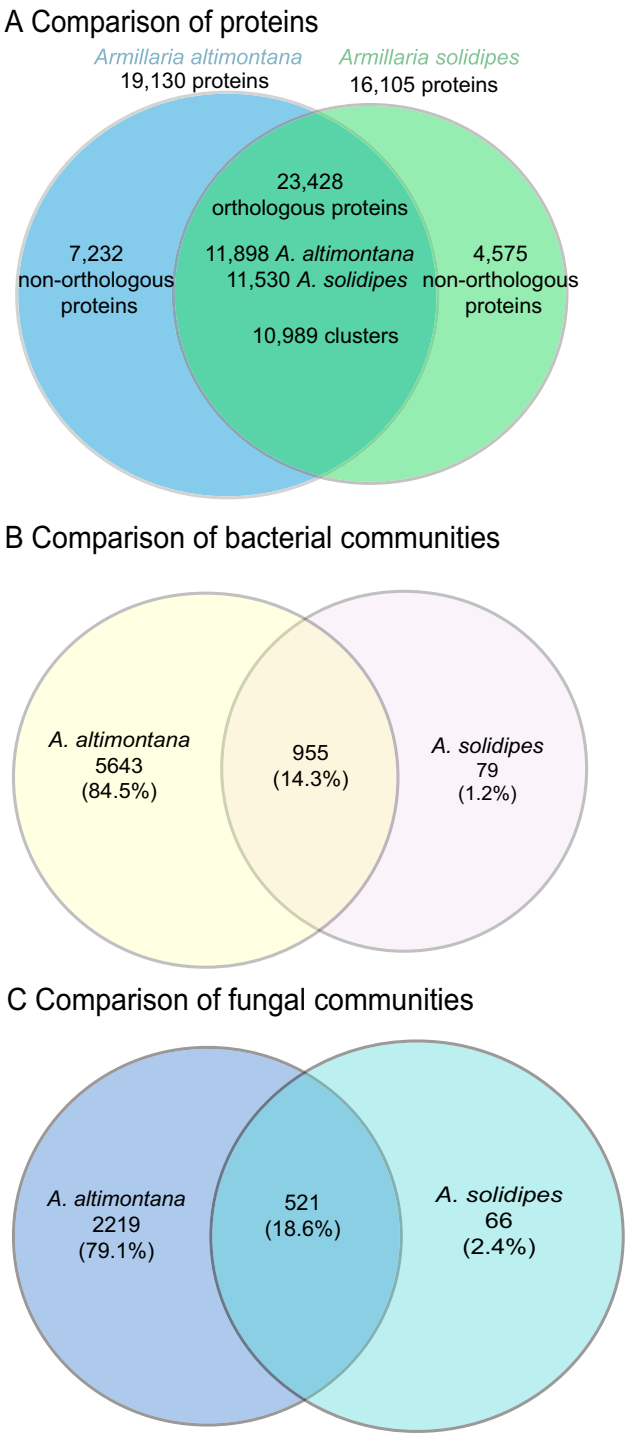

Fig. 5 **A** Orthologous and non-orthologous proteins of *Armillaria altimontana* and *A. solidipes*. **B**, **C** Microbial communities (OTUs) between *A. altimontana* and *A. solidipes*. The core microbiome encompasses overlap between both species, while unique OTUs occur within each circle for bacterial communities (**B**) and fungal communities (**C**)

processing was 27,639 reads/sample, with a range from 6 to 107,582. Eighteen samples yielded < 5000 total reads and were removed from analyses for the 16S dataset. For the ITS dataset, the mean sequencing depth after processing was 51,806 reads/sample, with a range from 15,017 to 77,969. The total datasets yielded 26,781 and 6936 OTUs for the 16S and ITS2, respectively. The resulting rarefaction curves for these 16S sequence data indicate adequate sampling depth (Fig. S3). Matching to the Silva database resulted in a 16S dataset of 6677 unique OTUs, and matching to the UNITE database resulted in an ITS2 dataset of 2806 unique OTUs.

Differences in Community Alpha Diversity and Richness

Bacterial and fungal communities were assessed for overall rarefied richness and diversity (Fig. S3). We did not observe significant differences in richness among soil fungal communities associated with *A. solidipes* or *A. altimontana* ($F_{(1,52)} = 0.0462$, $P = 0.8310$). Additionally, we did not observe significant fungal differences for either diversity index (Shannon's or inverse Simpson) associated with *A. solidipes* or *A. altimontana* ($F_{(1,52)} = 0.16$, $P = 0.6910$; $F_{(1,52)} = 0.5729$, $P = 0.4530$; Table S2). Although not statistically significant, soils associated with *A. solidipes* had greater fungal richness and diversity, compared to *A. altimontana*. Bacterial richness measurements indicated that soils associated *Armillaria* species were slightly significant ($F_{(1,34)} = 3.905$, $P = 0.0563$) with *A. altimontana* having greater richness. For both diversity indices, soils associated with *A. altimontana* had greater bacterial community diversity. Shannon's diversity was slightly significant ($F_{(1,34)} = 4.0619$, $P = 0.0518$), though the inverse Simpson index was not significant between *Armillaria* species ($F_{(1,34)} = 1.4005$, $P = 0.2448$; Table S2).

Additionally, *A. altimontana* had a slightly significant positive relationship ($P = 0.053$) and soil moisture had a significant negative relationship ($P = 0.013$) with fungal richness (Table S3). In the diversity analyses, the Shannon's diversity model was not significant ($P = 0.489$), while *A. altimontana* ($P = 0.067$; positive) and soil moisture ($P = 0.078$; negative) both had an influence on diversity. No edaphic variables significantly correlated to inverse Simpsons diversity measures across fungal communities ($P = 0.558$; Table S3). Soil moisture had a significant negative relationship with bacterial richness ($P = 0.049$; Table S4). Both *A. solidipes* ($P = 0.039$) and soil moisture ($P = 0.022$) had a significant negative relationship with bacterial Shannon's diversity. The bacterial inverse Simpson diversity model was significant ($P = 0.0423$), with soil moisture ($P = 0.024$, negative) as the lone significant predictor (Table S4).

Table 5 Number of orthologous and non-orthologous proteins in *Armillaria altimontana* and *A. solidipes*. Only information for proteins with count differences > 5 were included, except for non-orthologous terpene synthase and transcriptional activator of glycolytic enzymes for which only four were present in *A. altimontana*

Orthologous proteins[a]				
Cluster_name	Protein number	Annotation	*A. altimontana*	*A. solidipes*
Cluster 1	30	Transposase	28	2
Cluster 6	19	BTB/POZ domain protein, maybe transcription factor	18	1
Cluster 12	16	CBM67, rhamnose binding in polysaccharides (pectin)	15	1
Cluster 13	16	Only one protein with: zinc knuckle domain	15	1
Cluster 2	21	Helicase, involved in telomere maintenance	15	6
Cluster 4	21	No annotation	14	7
Cluster 19	14	No annotation	13	1
Cluster 14	15	No annotation	13	2
Cluster 27	13	F-box domain protein, different functions including fungal pathogenesis	12	1
Cluster 31	12	No annotation	11	1
Cluster 30	12	ABC transporter	11	1
Cluster 24	13	No annotation	11	2
Cluster 53	10	No annotation	9	1
Cluster 55	10	Only one protein with: uncharacterized domain	9	1
Cluster 61	9	No annotation	8	1
Cluster 63	9	Transposase	8	1
Cluster 68	9	No annotation	8	1
Cluster 70	9	No annotation	8	1
Cluster 73	9	No annotation	8	1
Cluster 74	9	No annotation	8	1
Cluster 79	9	Helicase, involved in telomere maintenance	8	1
Cluster 54	10	No annotation	8	2
Cluster 44	10	SET domain protein, histone-modifying enzymes	8	2
Cluster 81	8	No annotation	7	1
Cluster 40	11	Only three proteins with: domain of unknown function	2	9
Cluster 10	19	F-box domain protein, different functions including fungal pathogenesis	2	17
Cluster 99	8	Caspase domain protein	1	7
Cluster 100	8	No annotation	1	7
Cluster 28	13	Caspase domain protein	1	12
Non-orthologous proteins				
Annotation	*A. altimontana*	*A. solidipes*		
CAZymes	91	80		
Cytochrome P450	87	48		
Other proteins with count difference > 5				
polyprenyl synthase	15	6		
trichodiene synthase	2	11		
F-box protein	81	52		
glutathione S-transferase	1	11		
Clp amino terminal domain, pathogenicity island component	6	0		
DDE superfamily endonuclease	8	0		
Sodium/hydrogen exchanger family	0	8		
Secreted proteins/small secreted proteins	344/327	265/248		

Table 5 (continued)

Exclusive with possible host-interaction function		
terpene synthase	4	0
transcriptional activator of glycolytic enzymes	4	0

[a]2 protein clusters = 10,321; 3–5 protein clusters = 576; > 5 protein cluster = 29

Bacterial and Fungal Beta Diversity

Principal components analysis (PCoA) was completed to quantify beta diversity between bacterial and fungal communities associated with each *Armillaria* species. Beta diversity associated with soil bacterial communities of *A. altimontana* and *A. solidipes* were not significantly different ($P = 0.544$), and this is observed in the PCoA plot (Fig. S4A). Axes 1 and 2 described 21.7 and 12% of the variation, respectively. We observed that beta diversity indices were significantly different for fungal soil communities associated with *Armillaria* species as well ($P = 0.016$) (Fig. S4B). Compared to the bacterial communities, axes 1 and 2 described less of the fungal variation at 9.67 and 7.25%, respectively.

Core Communities Associated with *Armillaria* Species

Venn diagrams were constructed to identify the individual and core bacterial and fungal communities (Fig. 5 A and B). Of the 6677 total OTUs, the core bacterial communities for soils associated with both *Armillaria* species consisted of 955 OTUs (14.3%). While a significant abundance, 5643 OTUs (84.5%), was uniquely associated with *A. altimontana*, only 79 (1.2%) were uniquely associated with *A. solidipes* (Fig. 5B). The core fungal community associated with both *A. altimontana* and *A. solidipes* consisted of 521 OTUs (18.6%). Far surpassing the core community, 2219 OTUs (79.1%) were unique to *A. altimontana*–associated soils, whereas only 66 (2.4%) OTUs were unique to *A. solidipes*–associated soils (Fig. 5C).

Taxonomic Trends and Relative Abundance

There were 17 16S bacterial families that exceeded the relative abundance of 1% (Fig. 6A). All 17 families were in soils associated with *A. altimontana*. Pseudomonadaceae was found in high abundance followed by Chthoniobacteraceae and Pyrinomonadaceae with *A. altimontana*. We observed a large relative abundance of Enterobacteriaceae, followed by Pseudomonadaceae with *A. solidipes* (Fig. 6A).

In total, 17 fungal families exceeded a relative abundance of 1% (Fig. 6B). Mortierellaceae was found in high abundance for both *A. altimontana* and *A. solidipes*. Although

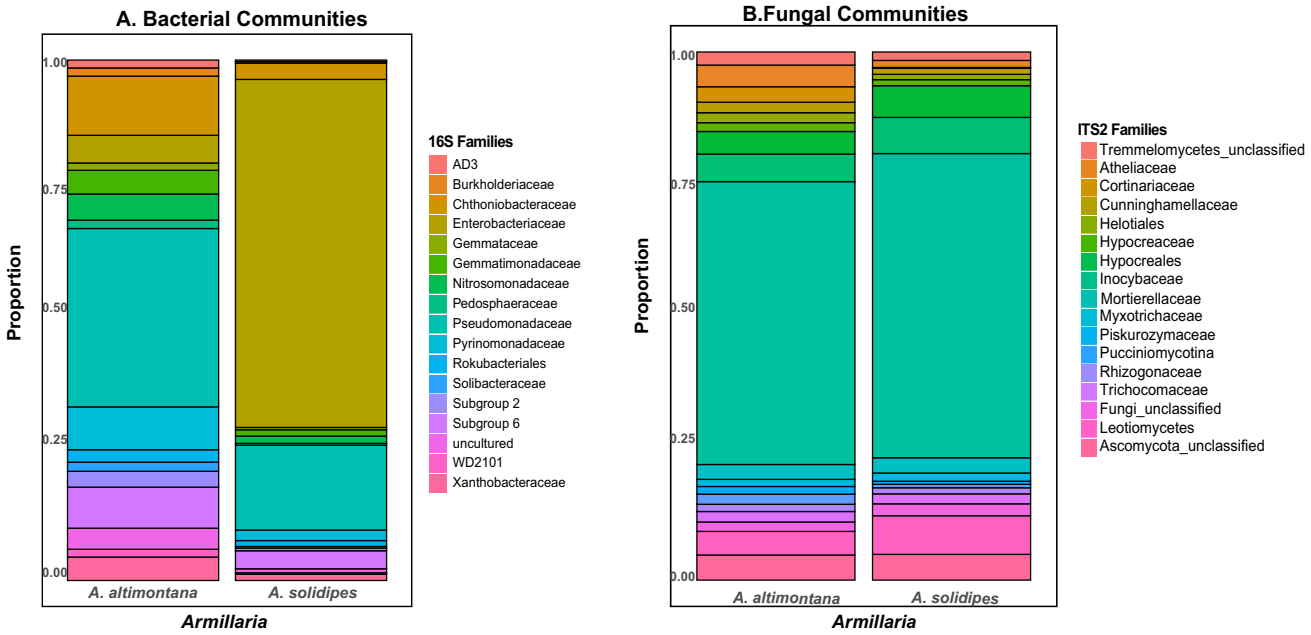

Fig. 6 Stacked bar graphs of top 17 most abundant bacterial families (**A**) and fungal families (**B**) for *Armillaria altimontana* and *A. solidipes*

not significant, fungal communities including Atheliaceae, Cortinariaceae, Helotiales, Hypocreaceae (e.g., *Trichoderma* spp.), Pucciniomycotina, and Rhizopogonaceae were more abundant in association with *A. altimontana*, whereas more Hypocreales, Inocybaceae, and Leotiomycetes were detected in soils associated with *A. solidipes* (Fig. 6B).

MetagenomeSeq analysis

We identified a total of four bacterial taxa that contributed significantly to the differential comparison between *Armillaria* species using the magnitude of OTU log-fold change (Fig. 7A). A proliferation, at 90% confidence, of Nitrosococcaceae (wb1-P19), Solirubrobacteraceae, Enterobacteriaceae, and Gammoproteobacteria_PLTA13_fa was found in *A. solidipes*–associated soils, whereas only uncultured bacteria were found to be significantly greater in *A. altimontana*–associated soils. We identified a total of five fungal taxa that contributed significantly to the comparison between *Armillaria* species using the magnitude of OTU log-fold change at the 90% confidence level (Fig. 7B). These analyses identified a proliferation of Atheliaceae, Suillaceae, Rhizopogonaceae, and unclassified fungi in *A. altimontana*–associated soils, whereas only a single OTU (unclassified fungi) was significantly more abundant in *A. solidipes*–associated soils.

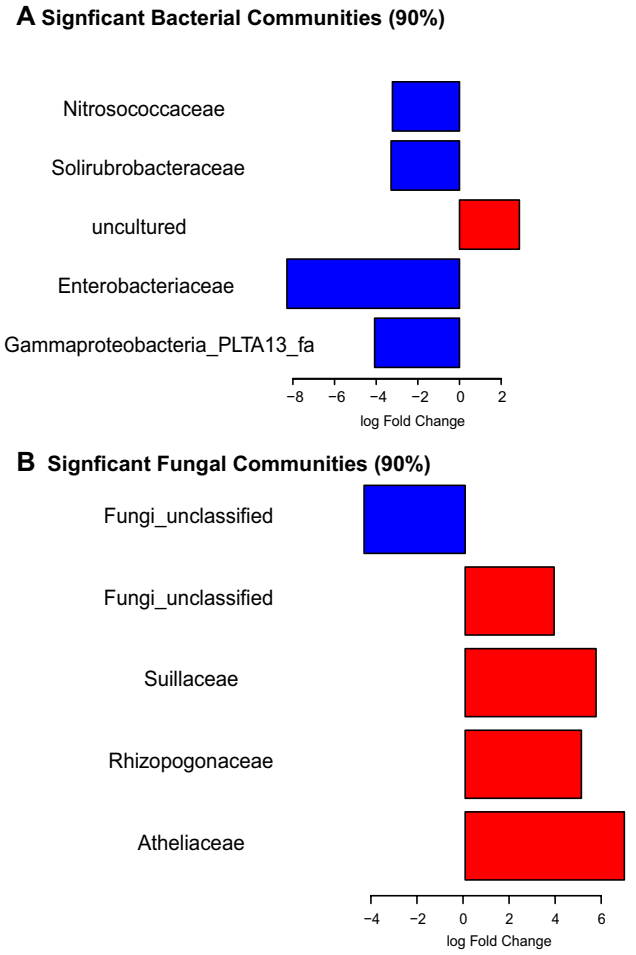

Fig. 7 Log fold change for unique bacterial (**A**) and fungal (**B**) OTUs in association between *A. altimontana* (red) and *A. solidipes* (blue). Significance is based on 90% confidence log fold change between both species of *Armillaria*

Discussion

We report the high-quality genome assemblies with structural and functional annotations for two *Armillaria* species (*A. altimontana* and *A. solidipes*) that display different ecological lifestyles. In addition, we examined the potential role and relationship among microbial communities that may correspond with the different ecological behaviors of *A. altimontana* and *A. solidipes*. *Armillaria* isolates were obtained from a conifer forest in northern Idaho within the interior western USA, where *A. altimontana* primarily behaves as a saprophyte and potentially beneficial biocontrol agent enhancing the growth/survival of western white pine [20] and *A. solidipes* primarily acts as an aggressive pathogen of diverse conifers [11, 13, 95]. In a whole-genome phylogenomic tree, *A. cepistipes* and *A. gallica*, which are often considered as weak or opportunistic pathogens, are closely related to *A. altimontana*. This result is similar to other published phylogenetic trees, where *A. altimontana* tends to group with less virulent pathogens (e.g., *A. cepistipes*, *A. calvescens*, *A. gallica*, and *A. nabsnona*) within the Gallica superclade, which is well separated from the *A. solidipes* group (e.g., *A. ostoyae*, *A. gemina*, and *A. sinapina*) within the Solidipes/Ostoyae superclade [22, 23, 96]. The phylogenetic placement of *A. altimontana*, compared to *A. mellea*, a virulent pathogen within Mellea superclade, which is ancestral to the Gallica superclade, suggests that perhaps *A. altimontana* is evolving towards lower virulence.

The genome assemblies presented here were similar in size to other *Armillaria* genomes assemblies, although our *A. solidipes* genome is smaller than the *A. solidipes/ostoyae* 28–4 genome of Anderson and Spatafora (58.01 Mbp; JGI web site); this could be attributable to the different sequencing technologies used (PacBio and Illumina, respectively) and/or different isolates sequenced. Both *A. solidipes* assemblies are, however, smaller than the *A. ostoyae* C18/9 (60.1 Mbp) assembly from Europe [28]. Although it has been proposed that *A. solidipes* and *A. ostoyae* are a single species [97], genomic differences result in a separate grouping for *A. ostoyae* (C18/9) from Europe, which is distinct from the two *A. solidipes* isolates from North America in the whole-genome phylogenetic tree. Thus, the phylogenomic analysis

further supports that North American *A. solidipes* is distinct from Eurasian *A. ostoyae*.

Armillaria altimontana has a larger genome and a proportionately larger number of protein-coding genes compared to *A. solidipes*. It had twice as many sequences coding for repetitive elements (18,346,415 bp) than *A. solidipes* (9,691,790 bp); however, this difference is less than would be accounted for from the larger genome size alone (73.7 Mbp versus 55.7 Mbp, respectively). Rather, it has been suggested that gene family expansion has driven the increase of genome sizes in *Armillaria* in comparison with other Agaricales [28], and this could also be the mechanism responsible for the expanded genomes of *A. altimontana*, *A. cepistipes* (75.5 Mbp), and *A. gallica* (85.3 Mbp). Nevertheless, the genomes of *A. altimontana* and *A. solidipes* shared large blocks of synteny (i.e., large blocks of gene order when comparing the two genomes) suggesting that their gene sets are similar within the genomes of two *Armillaria* species. Interestingly, *A. altimontana* genome encodes only slightly more secreted proteins, secreted CAZymes, ABC transporters, and secondary metabolite clusters, but with slightly fewer tRNA genes compared to *A. solidipes*. Though *A. altimontana* has a larger genome than *A. solidipes*, the genomes are similar in synteny and in gene content; however, *A. altimontana* contains considerably more predicted non-secreted proteins.

Although relatively few genomic differences were observed, genome signatures of lifestyle differences between *A. solidipes* and *A. altimontana* were highlighted by the variation in putative secreted proteins. Approximately 1200 encoded proteins in the two *Armillaria* genomes were found as potentially secreted, which could be potentially also considered as potential "effectors" — important proteins for interactions with a host [98]. Both species were well-equipped with genes encoding enzymes to degrade cell wall components, including cellulose, hemicellulose, lignin, pectin, proteins, and others. The major differences between the two *Armillaria* species are that *A. altimontana* had more carbohydrate-binding enzymes, beta-glucan-degrading enzymes, and more proteins predicted to be involvement in host interactions (hydrophobin, cerato-platanin), especially small secreted proteins [99]. In contrast, the genome of *A. solidipes* encoded more secreted putative cellulose, hemicellulose, pectin, and lignin-degrading enzymes. The combination of these secreted proteins could confer *A. solidipes* with a higher ability to infect and cause damage to its host. However, this hypothesis requires functional tests, because the number of CAZymes varies widely when comparing fungi with similar or different lifestyles [100]. Also, it has been found that phylogenetic history can have a more important influence on secretome composition than lifestyle [101].

We found that more than half of predicted proteins in *A. altimontana* and almost two-thirds of *A. solidipes* predicted proteins could be considered orthologous. Most of these clusters had very similar numbers of proteins that were encoded in the genome of each *Armillaria* species. In contrast, all *A. altimontana* CBM67 proteins (15) were in a cluster, with only one CBM67 protein encoded by *A. solidipes*. Of the 15 *A. altimontana* CBM67 proteins, 11 were predicted as secreted, as was the one *A. solidipes* CBM67 protein. CBM67 is one of several CBM considered "lectin-like," and we speculate that in *Armillaria* spp., CBM67 proteins may have an additional functionality other that help in pectin degradation, such as interactions with the host and other organisms [102], particularly in *A. altimontana* which contains more CBM67 genes.

Among non-orthologous proteins, another major difference was observed in the total numbers of gene encoding cytochrome P450 enzymes: *A. altimontana* had considerably more both non-orthologous cytochrome P450 genes and a higher total of all cytochrome P450 genes, which are known to be involved in numerous metabolic pathways and biological processes including degradation of lignin and xenobiotics, secondary metabolite synthesis, and adaptation to different environments [88–91]. The versatile activities of cytochrome P450 enzymes make it difficult to assign a specific function for them, but we speculate that a larger number of genes encoding these enzymes, including many non-orthologous enzymes, could be associated with different lifestyles, in this case more saprophytic lifestyle for *A. altimontana* and a more pathogenic lifestyle for *A. solidipes*. A recent report also found a larger number of genes coding for cytochrome P450 in the saprophytic *A. cepistipes* compared to the pathogenic *A. ostoyae* [103].

Although non-orthologous proteins could have the similar molecular functions, their sequence differences could change their interactions with their substrates, regulation, or environmental optima [104]. Furthermore, the expression levels and the timing of expression could account for important ecological differences in how the two *Armillaria* species interact with their hosts [103]. Variations in the expression of many genes, including some related to pathogenicity, have been observed even among strains of the same species, and these variations are associated with different levels of virulence during host infection [105].

Rhizomorphs are an important and unique means by which that *Armillaria* species interact with their environment, hosts, and substrates. Differences in microbial communities associated with each *Armillaria* species can perhaps be putatively attributed to genes encoding enzymes similar to those secondary metabolite synthesis enzymes previously identified in *Armillaria* species [28]. We observed some differences when comparing the number of genes upregulated in rhizomorphs in the two *Armillaria* species. For example, polyprenyl synthase genes involved in terpenoid synthesis were more abundant in *A. altimontana* compared to *A. solidipes*, whereas genes involved in the production of

trichodiene, a potential signaling molecule or mycotoxin [106], were more abundant in *A. solidipes*. In general, terpenoids can have many different structures and functions, which have been involved in the interaction between fungi and plants and other organisms [107–110]. Trichodiene, on the other hand, is the immediate precursor to a family of toxins that cause damage to plant hosts [111].

Although overall differences of soil microbial communities were not observed in association with the two *Armillaria* species, several bacterial taxa were more differentially abundant in soils associated with *A. solidipes*, and several fungal taxa were more differentially abundant in association with *A. altimontana*. We identified the most significant logfold change of three Proteobacteria taxa within the Gammaproteobacteria class and Enterobacteriaceae in association with *A. solidipes*. Interestingly, one of these included Nitrosococcaceae wb1-P19, which is thought to be a nitrite-oxidizing autotrophic bacteria and that has previously been observed in caves [112–114]. In contrast, Gammaproteobacteria PLTA13_fa was found in high numbers in a Mn oxide-producing biofilm [115]. With these unique characteristics, it is not unexpected that some taxa within Proteobacteria have been characterized in soils contaminated with pesticides [116]. A recent study examining healthy ginseng (*Panax ginseng*) and ginseng with rusty root disease also found that several Proteobacteria were found in high abundances among diseased plants [117], and increases in Proteobacteria were also observed in association with changes of cover types from forest to grasslands in Hawai'i [118]. In addition, Enterobacteriaceae taxa have been associated with higher levels of Fusarium wilt disease of banana [119], but these taxa were also found in higher levels in asymptomatic Kauri trees compared to those infected with *Phytophthora agathidicida* [120]. Similar to our study, however, Byers et al. [120] found that Solirubrobacterales were more abundant with trees in decline. Przemieniecki et al. [121] surveyed bacterial communities associated *A. ostoyae* rhizomorphs during three stages of tree decline. They observed that rhizomorphs that were rich in Parabacteroides, *Clostridium*, and *Bacillus* were able to hydrolyze diverse organic compounds that could assist *Armillaria* rhizomorph enzymes in wood decomposition. Though these taxa were not present in our study, the high abundance of several taxa in the Proteobacteria and Enterobacteriaceae suggests potential recruitment of bacterial taxa by *A. solidipes* to assist in wood degradation. Alternatively, these results could suggest that the abundance of these taxa may be associated with tree mortality and/or changes in the plant community due to the activity of *A. solidipes*. Furthermore, as the rhizosphere of the infected tree begins to degrade, these taxa may thrive because of their unique abilities to breakdown complex plant root materials. Several studies have observed changes in bacterial communities associated with declines in plant communities [122–124]. More research is needed better understand signaling among members of the pathobiome during tree decline that could foster changes in the associated bacterial communities.

We identified several fungal taxa that were more significantly more abundant in association with *A. altimontana*. Several of these taxa have been shown to increase plant productivity through multiple functions, such as ectomycorrhizal fungi including Atheliaceae, Rhizopogonaceae, and Suillaceae [125–128]. Taxa from all three ectomycorrhizal fungal families were significantly more differentially abundant in soils associated with *A. altimontana* compared to *A. solidipes*, allowing increased uptake of water and nutrients to enhance tree defenses against root diseases [31]. The functions of these *A. altimontana*–associated soil fungi suggest that these fungal communities may also contribute to the overall health of the forest stand, corroborating Warwell et al. [20], who found that trees associated with *A. altimontana* were larger in both diameter and height than trees not associated with this *Armillaria* species. It remains unknown if *A. altimontana* is conducive to mycorrhizal fungi though evidence provided herein suggests that *A. altimontana* co-occurs with mycorrhizal fungi.

Utilizing the naturally occurring soil fungal communities to assist in the management of Armillaria root disease may be key to long-term protection of residual trees on sites infested with pathogenic *Armillaria* spp., such as following Armillaria root disease–associated mortality or silvicultural thinning practices. Beneficial microbes can minimize pathogen inoculum loads by reducing pathogen growth or inhibiting pathogen infection of susceptible hosts [41]. In this study, a greater diversity of mycorrhizal and saprophytic fungi was observed in association with the beneficial/non-pathogenic *A. altimontana*, demonstrating that mycorrhizae may have a direct influence on hosts within forested environments associated with *Armillaria* species [125].

Selecting trees to sample *Armillaria* species was the greatest limiting factor in this study. More than 25 years before this study, *A. solidipes* was well represented on the site [20]. The small number of *A. solidipes*–infected trees in this study perhaps reflects the protective role of *A. altimontana* and the associated microbial community in suppressing *A. solidipes*; however, additional studies and surveys are needed to support this hypothesis. The survey approaches used in our study yielded rhizomorphs for 78% of the trees and adequate DNA from 90% of the samples. Additionally, the use of metatranscriptomics could further our understanding of the fungal microbes and their ecological functions within the soils associated with *A. altimontana* and *A. solidipes*.

In conclusion, we found high similarity comparing the genomes of between the beneficial/non-pathogenic *A. altimontana* and pathogenic *A. solidipes*. The larger number

of proteins encoded within *A. altimontana* genome results from moderate increases across many different gene families instead of a large expansion of a few gene families. However, we found many relatively small differences in genes that could contribute to differences in ecological lifestyles and interactions with woody hosts and soil microbes (fungi and bacteria). We did observe, however, that soil microbial communities may act in concert with *A. altimontana* to produce suppressive soils that help protect trees from Armillaria root disease, caused by *A. solidipes*. This study further suggests that novel approaches for managing Armillaria root disease could be based on management practices that favor naturally occurring, non-pathogenic *Armillaria* spp. and other beneficial soil microbes that suppress Armillaria root disease. Additionally, continued observations of microbial communities in association *Armillaria* spp. will provide additional insights on microbial changes over time in relation with Armillaria root disease and changing forest environments.

Supplementary Information The online version contains supplementary material available at https://doi.org/10.1007/s00248-022-01989-8.

Author Contribution All authors contributed to the study conception and design. Material preparation and data collection were performed by Bradley Lalande, John Hanna, Mee-Sook Kim, Ned Klopfenstein, and Jane Stewart. Analyses were performed by Jorge Ibarra Caballero, Bradley Lalande, and Jane Stewart. The first draft of the manuscript was written by Jorge Ibarra Caballero, Bradley Lalande, and Jane Stewart, and all authors commented on previous versions of the manuscript. All authors read and approved the final manuscript.

Funding This study was funded in part by the USDA Forest Service, State & Private forestry, Forest Health Protection, Special Technology Development Program and Joint Venture Agreements (19-JV-11221633–093 and 20-JV-11221633–141) to Colorado State University (JES).

Data Availability The datasets generated and/or analyzed during the current study are available in the NCBI database. The corresponding genome assemblies were deposited at the NCBI with accession number JAIWYR000000000 for *Armillaria altimontana*, and JAIWYQ000000000 for *A. solidipes*, and microbial dataset is in NCBI SRA database under accession number PRJNA767898.

Declarations

Compliance with Ethical Standards For this type of study, formal consent is not required.

Conflict of Interest The authors declare no competing interests.

References

1. Hess J, Skrede I, Chaib De Mares M, Hainaut M, Henrissat B, Pringle A (2018) Rapid divergence of genome architectures following the origin of an ectomycorrhizal symbiosis in the gene Amanita. Mol Biol Evol 35:2786–2804. https://doi.org/10.1093/molbev/msy179
2. Möller M, Stukenbrock EH (2017) Evolution and genome architecture in fungal plant pathogens. Nat Rev Microbiol 15:756–771. https://doi.org/10.1038/nrmicro.2017.76
3. Ryberg M, Matheny PB (2012) Asynchronous origins of ectomycorrhizal clades of Agaricales. Proc R Soc B 279:2003–2011. https://doi.org/10.1098/rspb.2011.2428
4. Tedersoo L, May TW, Smith ME (2010) Ectomycorrhizal lifestyle in fungi: global diversity, distribution, and evolution of phylogenetic lineages. Mycorrhiza 20:217–263. https://doi.org/10.1007/s00572-009-0274-x
5. Kohler A, Kuo A, Nagy L et al (2015) Convergent losses of decay mechanisms and rapid turnover of symbiosis genes in mycorrhizal mutualists. Nat Genet 47:410–415. https://doi.org/10.1038/ng.3223
6. Veneault-Fourrey C, Commun C, Kohler A, Morin E, Balestrini R, Plett J, Danchin E, Coutinho P, Wiebenga A, DeVries RP, Henrissat B, Martin F (2014) Genomic and transcriptomic analysis of *Laccaria bicolor* CAZome reveals insights into polysaccharides remodelling during symbiosis establishment. Fungal Genet Biol 72:168–181. https://doi.org/10.1016/j.fgb.2014.08.007
7. Dalman K, Himmelstrand K, Olson A, Lind M, Brandström-During M, Stenlid J (2013) A genome-wide association study identifies genomic regions for virulence in the non-model organism Heterobasidion annosum s.s. PLoSOne. 8:e53525. https://doi.org/10.1371/journal.pone.0053525
8. Zeng Z, Sun H, Vainio EJ, Raffaello T, Kovalchuk A, Morin E, Duplessis S, Asiegbu FO (2018) Intraspecific comparative genomics of isolates of the Norway spruce pathogen (*Heterobasidion parviporum*) and identification of its potential virulence factors. BMC Genomics 19:220. https://doi.org/10.1186/s12864-018-4610-4
9. Castanera R, Borgognone A, Pisbarro AG, Ramírez L (2017) Biology, dynamics and applications of transposable elements in basidiomycete fungi. Appl Microbiol Biotechnol 101:1337–1350. https://doi.org/10.1007/s00253-017-8097-8
10. Marçais B, Bréda N (2006) Role of an opportunistic pathogen in the decline of stressed oak trees. J Ecol 94:1214–1223. https://doi.org/10.1111/j.1365-2745.2006.01173.x
11. Baumgartner K, Coetzee MPA, Hoffmeister D (2011) Secrets of the subterranean pathosystem of *Armillaria*. Mol Plant Pathol 12:515–534. https://doi.org/10.1111/j.1364-3703.2010.00693.x
12. Cleary MR, van der Kamp BJ, Morrison DJ (2012) Pathogenicity and virulence of *Armillaria sinapina* and host response to infection in Douglas-fir, western hemlock and western redcedar in the southern Interior of British Columbia. Forest Pathol 42:481–491. https://doi.org/10.1111/j.1439-0329.2012.00782.x
13. Heinzelmann R, Prospero S, Rigling D (2017) Virulence and stump colonization ability of *Armillaria borealis* on Norway spruce seedlings in comparison to sympatric *Armillaria* species. Plant Dis 101:470–479. https://doi.org/10.1094/PDIS-06-16-0933-RE
14. Morrison DJ, Pellow KW (2002) Variation in virulence among isolates of *Armillaria ostoyae*. Forest Pathol 32:99–107. https://doi.org/10.1046/j.1439-0329.2002.00275.x
15. Morrison DJ (2004) Rhizomorph growth habit, saprophytic ability and virulence of 15 *Armillaria* species. Forest Pathol 34:15–26. https://doi.org/10.1046/j.1439-0329.2003.00345.x
16. Prospero S, Holdenrieder O, Rigling D (2004) Comparison of the virulence of *Armillaria cepistipes* and *Armillaria ostoyae* on four Norway spruce provenances. Forest Pathol 34:1–14. https://doi.org/10.1046/j.1437-4781.2003.00339.x
17. Brazee NJ, Ortiz-Santana B, Banik MT, Lindner DL (2012) *Armillaria altimontana*, a new species from the western interior of North America. Mycologia 104(5):1200–1205. https://doi.org/10.3852/11-409

18. Ferguson BA, Dreisbach TA, Parks CG, Filip G, Schmitt CL (2003) Coarse-scale population structure of pathogenic *Armillaria* species in a mixed conifer forest in the Blue Mountains of northeast Oregon. Can J For Res 33:612–633. https://doi.org/10.1139/x03-065
19. Kim M-S, Klopfenstein NB, McDonald GI, Arumuganathan K, Vidaver AK (2000) Characterization of North America *Armillaria* species by nuclear DNA content and RFLP analysis. Mycologia 92:874–883. https://doi.org/10.1080/00275514.2000.12061232
20. Warwell MV, McDonald GI, Hanna JW, Kim MS, Lalande BM, Stewart JE, Hudak AT, Klopfenstein NB (2019) *Armillaria altimontana* is associated with healthy western white pine (*Pinus monticola*): potential *in situ* biological control of Armillaria root disease pathogen, *A. solidipes*. Forests.10:294. https://doi.org/10.3390/f10040294
21. Rizzo DM, Harrington TC (1993) Delineation and biology of clones of *Armillaria ostoyae*, *A. gemina* and *A. calvescens*. Mycologia, 85(2):164-174. https://doi.org/10.2307/3760452.
22. Klopfenstein NB, Stewart JE, Ota Y, Hanna JW, Richardson BA, Ross-Davis AL, Elías-Román RD, Korhonen K, Keča N, Iturritxa E, Alvarado-Rosales D, Solheim H, Brazee NJ, Łakomy P, Cleary MR, Hasegawa E, Kikuchi T, Garza-Ocañas F, Tsopelas P, Rigling D, Prospero S, Tsykun T, Bérubé JA, Stefani FOP, Jafarpour S, Antonín V, Tomšovský M, McDonald GI, Woodward S, Kim MS (2017) Insights into the phylogeny of Northern Hemisphere Armillaria: neighbor-net and Bayesian analyses of translation elongation factor 1-α gene sequences. Mycologia 109:75–91. https://doi.org/10.1080/00275514.2017.1286572
23. Koch RA, Wilson AW, Séné O, Henkel TW, Aime MC (2017) Resolved phylogeny and biogeography of the root pathogen Armillaria and its gasteroid relative, Guyanagaster. BMC Evolutionary Biology. 17:33–48. https://doi.org/10.1186/s12862-017-0877-3
24. Heinzelmann R, Dutech C, Tsykun T, Labbé F, Soularue J-P, Prospero S (2019) Latest advances and future perspectives in *Armillaria* research. Can J Plant Path 41:1–23. https://doi.org/10.1080/07060661.2018.1558284
25. Devkota P, Hammerschmidt R (2020) The infection process of *Armillaria mellea* and *Armillaria solidipes*. Physiol Mol Plant Pathol 112:101543. https://doi.org/10.1016/j.pmpp.2020.101543
26. Collins C, Keane TM, Turner DJ, O'Keefe G, Fitzpatrick DA, Doyle S (2013) Genomic and proteomic dissection of the ubiquitous plant pathogen, *Armillaria mellea*: toward a new infection model system. J Proteome Res 12:2552–2570. https://doi.org/10.1021/pr301131t
27. Ross-Davis AL, Stewart JE, Hanna JW, Kim M-S, Cronn R, Rai H, Richardson BR, McDonald GI, Klopfenstein NB (2013) Transcriptome characterization of an Armillaria root disease pathogen reveals candidate pathogenicity-related genes. Forest Pathol 43:468–477. https://doi.org/10.1111/efp.12056
28. Sipos G, Prasanna AN, Walter MC, O'Connor E, Bálint B, Krizsán K, Kiss B, Hess J, Varga T, Slot J, Riley R, Bóka B, Rigling D, Barry K, Lee J, Mihaltcheva S, LaButti K, Lipzen A, Waldron R, Moloney NM, Sperisen C, Kredics L, Vágvölgyi C, Patrignani A, Fitzpatrick D, Nagy I, Doyle S, Anderson JB, Grigoriev IV, Güldener U, Münsterkötter M, Nagy LG (2017) Genome expansion and lineage-specific genetic innovations in the forest pathogenic fungi *Armillaria*. Nat Ecol Evol 1:1931–1941. https://doi.org/10.1038/s41559-017-0347-8
29. Azul AM, Nunes J, Ferreira I, Coehlo AS, Verissmo P, Trovao J, Campos A, Castro O, Freitas H (2014) Valuing native ectomycorrhizal fungi as a Mediterranean forestry component for sustainable and innovative solutions. Botany 92:161–171. https://doi.org/10.1139/cjb-2013-0170
30. Baldrian P (2017) Forest microbiome: diversity, complexity, and dynamics. *FEMS* Microbiology Reviews. 41:109-130. https://doi.org/10.1093/femsre/fuw040
31. Leake J, Johnson D, Donnelly D, Muckle G, Boddy L, Read D (2004) Networks of power and influence: the role of mycorrhizal mycelium in controlling plant communities and agroecosystem functioning. Can J Bot 82:1016–1045. https://doi.org/10.1139/b04-060
32. Lee Taylor D, Sinsabaugh RL (2014) Chapter 4: the soil fungi: occurrence, phylogeny, and ecology. In E.A. Paul (4th ed.), *Soil microbiology, ecology and biochemistry*. Cambridge, MA: Academic Press. p. 339–382. eBook ISBN: 9780123914118. https://doi.org/10.1016/C2011-0-05497-2.
33. Saif SR, Khan AG (1975) The influence of season and stage of development of plant on endogone mycorrhiza of field-grown wheat. Can J Microbiol 82:1020–1024. https://doi.org/10.1139/m75-151
34. Cardenas E, Kranabetter JM, Hope G, Maas KR, Hallam S, Mohn WM (2015) Forest harvesting reduces the soil metagenomic potential for biomass decomposition. ISME 9:2465–2476. https://doi.org/10.1038/ismej.2015.57
35. Chapman SK, Koch GW (2007) What type of diversity yields synergy during mixed litter decomposition in a natural forest ecosystem? Plant Soil 299:153–162. https://doi.org/10.1007/s11104-007-9372-8
36. Davidson EA, Janssens IA (2006) Temperature sensitivity of soil carbon decomposition and feedbacks to climate change. Nature 440:165–173. https://doi.org/10.1038/nature04514
37. Robertson GP, Groffman PM (2014) Chapter 14: nitrogen transformation. In E.A. Paul (4th ed.), *Soil microbiology, ecology and biochemistry*. Cambridge, MA: Academic Press. p. 339–382. eBook ISBN: 9780123914118. https://doi.org/10.1016/C2011-0-05497-2.
38. Schloter M, Dilly O, Munch JC (2003) Indicators for evaluating soil quality. Agr Ecosyst Environ 98:255–262. https://doi.org/10.1016/S0167-8809(03)00085-9
39. Allison SD, Martiny JBH (2008) Resistance, resilience, and redundancy in microbial communities. PNAS 105(1):11512–11519. https://doi.org/10.1073/pnas.0801925105
40. Horwath W (2014) Chapter 12: carbon cycling: the dynamics and formation of organic matter. In E.A. Paul (4th ed.), *Soil microbiology, ecology and biochemistry*. Cambridge, MA: Academic Press. p. 339–382. eBook ISBN: 9780123914118. https://doi.org/10.1016/C2011-0-05497-2.
41. Kile GA, McDonald GI, Byler JW (1991) Ecology and disease in natural forests. In: C.G. Shaw and G.A. Kile, Armillaria root disease. United States Department of Agriculture Forest Service. Agricultural Handbook No. 691. Washington D.C. p. 102–121.
42. Kim MS, Ross-Davis AL, Stewart JE, Hanna JW, Warwell MV, Zambino PJ, Cleaver C, McDonald GI, Page-Dumroese DS, Moltzan B, Klopfenstein NB (2016) Can metagenomic studies of soil microbial communities provide novel insights toward developing novel management approaches for Armillaria root disease? Ramsey, A. and Palacios, P., compilers. Proceedings of the 63rd annual Western International Forest Disease Work Conference, Sept. 21–25, 2015. Newport, OR, USA.
43. Stewart JE, Kim M-S, Lalande, BM, Klopfenstein NB (2021) Pathobiome and microbial communities associated with forest tree root diseases [Chapter 15]. In: Asiegbu, Fred O.; Kovalchuk, Andriy, eds. Forest microbiology - tree microbiome: phyllosphere, endosphere, and rhizosphere, Volume 1. London, UK: Academic Press, Elsevier, Inc. p. 277–292. https://doi.org/10.1016/C2019-0-03562-5.
44. Kedves O, Shahab D, Champramary S, Chen L, Indic G, Bóka B, Nagy VD, Vágvölgyi C, Kredics L, Sipos G (2021) Epidemiology, biotic interactions, and biological control of armillarioids

in the Northern Hemisphere. Pathogens 10:76. https://doi.org/10.3390/pathogens10010076
45. Ross-Davis A, Settles M, Hanna JW, Shaw JD, Hudak AT, Page-Dumroese DS, Klopfenstein NB (2015) Using a metagenomic approach to improve our understanding of Armillaria root disease. pp. 73–78 in: Murray, M. and Palacios, P., compilers. Proceedings of the 62nd annual Western International Forest Disease Work Conference, Sept. 8–12, 2014. Cedar City, UT, USA.
46. Gurevich A, Saveliev V, Vyahhi N, Tesler G (2013) QUAST: quality assessment tool for genome assemblies. Bioinformatics 29(8):1072–1075. https://doi.org/10.1093/bioinformatics/btt086
47. Simão FA, Waterhouse RM, Ioannidis P, Kriventseva EV, Zdobnov EM (2015) BUSCO: assessing genome assembly and annotation completeness with single-copy orthologs. Bioinformatics 31(19):3210–3212. https://doi.org/10.1093/bioinformatics/btv351
48. Bertels F, Silander OK, Pachkov M, Rainey PB, van Nimwegen E (2014) Automated reconstruction of whole genome phylogenies from short sequence reads. Mol Biol Evol 31(5):1077–1088. https://doi.org/10.1093/molbev/msu088
49. Langmead B, Salzberg SL (2012) Fast gapped-read alignment with Bowtie 2. Nat Methods 9:357–359. https://doi.org/10.1038/nmeth.1923
50 Guindon S, Dufayard JF, Lefort V, Anisimova M, Hordijk W, Gascuel O (2010) New algorithms and methods to estimate maximum-likelihood phylogenies: assessing the performance of PhyML 3.0. Systematic Biology. 59(3):307–21. https://doi.org/10.1093/sysbio/syq010
51. Smit AFA, Hubley R (2015) RepeatModeler Open-1.0. 2013–2015. Available from: www.repeatmasker.org. Accessed Mar 2021
52. Cantarel BL, Korf I, Robb SMC, Parra G, Ross E, Moore B, Holt C, Sánchez Alvarado A, Yandell M (2008) MAKER: an easy-to-use annotation pipeline designed for emerging model organism genomes. Genome Res 18(1):188–196. https://doi.org/10.1101/gr.6743907
53. Smit AR, Hubley R, Green P (2013) RepeatMasker Open-4.0. http://www.repeatmasker.org. Accessed Mar 2021
54. Keller O, Kollmar M, Stanke M, Waack S (2011) A novel hybrid gene prediction method employing protein multiple sequence alignments. Bioinformatics 27(6):757–763. https://doi.org/10.1093/bioinformatics/btr010
55. Ter-Hovhannisyan V, Lomsadze A, Chernoff Y, Borodovsky M (2008) Gene prediction in novel fungal genomes using an ab initio algorithm with unsupervised training. Genome Res 18:1979–1990. https://doi.org/10.1101/gr.081612.108
56. Zaharia M, Bolosky WJ, Curtis K, Fox A, Patterson D, Shenker S, Stoica I, Karp RM, Sittler T (2011) Faster and more accurate sequence alignment with SNAP. arXiv:1111.5572v1.
57. Lowe TM, Eddy SR (1997) tRNAscan-SE: a program for improved detection of transfer RNA genes in genomic sequence. Nucleic Acids Res 25:955–964. https://doi.org/10.1093/nar/25.5.955
58. Camacho C, Coulouris G, Avagyan V, Ma N, Papadopoulos J, Bealer K, Madden TL (2009) BLAST+: architecture and applications. BMC Bioinformatics 10:421–429. https://doi.org/10.1186/1471-2105-10-421
59. Jones P, Binns D, Chang H, Fraser M, Li W, McAnulla C, McWilliam H, Maslen J, Mitchell A, Nuka G, Pesseat S, Quinn AF, Sangrador-Vegas A, Scheremetjew M, Yong S, Lopez R, Hunter S (2014) InterProScan 5: genome-scale protein function classification. Bioinformatics 30(9):1236–1240. https://doi.org/10.1093/bioinformatics/btu031
60. Zhang H, Yohe T, Huang L, Entwistle S, Wu P, Yang Z, Busk PK, Xu Y, Yin Y (2018) dbCAN2: a meta server for automated carbohydrate-active enzyme annotation. Nucleic Acids Res 46:W95–W101. https://doi.org/10.1093/nar/gky418
61. Urban M, Cuzick A, Seager J, Wood V, Rutherford K, Venkatesh SY, De Silva N, Martinez MC, Pedro H, Yates AD, Hassani-Pak K, Hammond-Kosack KE (2020) PHI-base: the pathogen–host interactions database. Nucleic Acids Res 48:D613–D620. https://doi.org/10.1093/nar/gkz904
62. Blin K, Shaw S, Steinke K, Villebro R, Ziemert N, Lee SY, Medema MH, Weber T (2019) antiSMASH 5.0: updates to the secondary metabolite genome mining pipeline. Nucleic Acids Research. Volume 47, Issue W1:W81–W87. https://doi.org/10.1093/nar/gkz310.
63. Almagro Armenteros JJ, Sønderby CK, Sønderby SK, Nielsen H, Winther O (2017) DeepLoc: prediction of protein subcellular localization using deep learning. Bioinformatics 33:3387–3395. https://doi.org/10.1093/bioinformatics/btx431
64. Soderlund C, Nelson W, Shoemaker A, Paterson A (2006) SyMAP: a system for discovering and viewing syntenic regions of FPC maps. Genome Res 16:1159–1168. https://doi.org/10.1101/gr.5396706
65. Soderlund C, Bomhoff M, Nelson W (2011) SyMAP: a turnkey synteny system with application to plant genomes. Nucleic Acids Res 39(10):e68. https://doi.org/10.1093/nar/gkr123
66. Xu L, Dong Z, Fang L, Luo Y, Wei Z, Guo H, Zhang G, Gu YQ, Coleman-Derr D, Xia Q, Wang Y (2019) OrthoVenn2: a web server for whole-genome comparison and annotation of orthologous clusters across multiple species. Nucleic Acids Res 47:W52–W58. https://doi.org/10.1093/nar/gkz333
67. Rehner SA, Buckley E (2005) A Beauveria phylogeny inferred from nuclear ITS and EF1-a sequences: evidence for cryptic diversification and links to Cordyceps teleomorphs. Mycologia 97:84–98. https://doi.org/10.3852/mycologia.97.1.84
68. White TJ, Bruns T, Taylor J (1990) Amplification and direct sequencing of fungal ribosomal RNA genes for phylogenetics. In: *A guide to molecular methods and applications* (Innis MA, Gelfand DH, Sninsky JJ, White JW, eds). Academic Press, New York: 315–322. https://doi.org/10.1016/B978-0-12-372180-8.50042-1.
69. Walters W, Hyde ER, Berg-Lyons D, Ackermann G, Humphrey G, Parada A, Gilbert JA, Jansson JK, Caporaso JG, Fuhrman JA, Apprill A, Knight B (2015) Improved bacterial 16S rRNA gene (V4 and V4–5) and fungal internal transcribed spacer marker gene primers for microbial community surveys. mSystems 1(1):e00009–15. doi: https://doi.org/10.1128/mSystems.00009-15.
70. Bolger AM, Lohse M, Usadel B (2014) Trimmomatic: a flexible trimmer for Illumina sequence data. Bioinformatics 30:2114–2120. https://doi.org/10.1093/bioinformatics/btu170
71. Schloss PD, Westcott SL, Ryabin T, Hall JR, Hartmann M, Hollister EB, Lesniewski RA, Oakley BB, Parks DH, Robinson CJ, Sahl JW, Stres B, Thallinger GG, Van Horn DJ, Weber CF (2009) Introducing mothur: open-source, platform-independent, community-supported software for describing and comparing microbial communities. Appl Environ Microbiol 75:7537–7541. https://doi.org/10.1128/AEM.01541-09
72. Kozich JJ, Westcott SL, Baxter NT, Highlander SK, Schloss PD (2013) Development of a dual-index sequencing strategy and curation pipeline for analyzing amplicon sequence data on the MiSeq Illumina sequencing platform. Appl Environ Microbiol 79:5112–5120. https://doi.org/10.1128/AEM.01043-13
73. Edgar RC, Haas BJ, Clemente JC, Quince C, Knight R (2011) UCHIME improves sensitivity and speed of chimera detection. Bioinformatics 27:2194–2200. https://doi.org/10.1093/bioinformatics/btr381

74. Edgar RC (2010) Search and clustering orders of magnitude faster than BLAST. Bioinformatics 26(19):2460–2461. https://doi.org/10.1093/bioinformatics/btq461
75. Quast C, Pruesse E, Yilmaz P, Gerken J, Schweer T, Yarza P, Peplies J, Glöckner FO (2013) The SILVA ribosomal RNA gene database project: improved data processing and web-based tools. Nucleic Acid Res 41:D590–D596. https://doi.org/10.1093/nar/gks1219
76. Nilsson RH, Larsson K-H, Taylor AFS, Bengtsson-Palme J, Jeppesen JS, Schigel D, Kennedy P, Picard K, Glöckner FO, Tedersoo L, Saar I, Kõljalg U, Abarenkov K (2019) The UNITE database for molecular identification of fungi: handling dark taxa and parallel taxonomic classifications. Nucleic Acids Res 47:D259–D264. https://doi.org/10.1093/nar/gky1022
77. Wang Q, Garrity GM, Tiedje JM, Cole JR (2007) Naïve Bayesian classifier for rapid assignment of rRNA sequences into the new bacterial taxonomy. Appl Environ Microbiol 73:5261–5267. https://doi.org/10.1128/AEM.00062-07
78. Oksanen J, Blanchet FG, Friendly M, Kindt R, Legendre P, McGlinn D, Minchin PR, O'Hara RB, Simpson GL, Solymos P, Stevens MHH, Szoecs E, Wagner H (2017) vegan: Community Ecology Package. R package version 2.4–2.
79. Olofsson TC, Vásquez A (2008) Detection and identification of a novel lactic acid bacterial flora within the honey stomach of the honeybee *Apis mellifera*. Curr Microbiol 57:356–363. https://doi.org/10.1007/s00284-008-9202-0
80. Hill TCJ, Walsh KA, Harris JA, Moffett BF (2006) Using ecological diversity measures with bacterial communities. FEMS Microbiol Ecol 43:1–11. https://doi.org/10.1111/j.1574-6941.2003.tb01040.x
81. Nagendra H (2002) Opposite trends in response to Shannon and Simpson indices of landscape diversity. Appl Geogr 22:175–186. https://doi.org/10.1016/S0143-6228(02)00002-4
82. Zhang H, John R, Peng Z, Yuan J, Chu C, Du G, Zhou S (2012) The relationship between species richness and evenness in plant communities along a successional gradient: a study from sub-alpine meadows of the eastern Qinghai-Tibetan Plateau. China PLoS ONE 7:e49024. https://doi.org/10.1371/journal.pone.0049024
83. Paulson JN, Talukder H, Pop M, Bravo HC (2021) metagenomeSeq: statistical analysis for sparse high-throughput sequencing. Bioconductor package: 1.16.0.
84. Wickham H (2016) *ggplot2: elegant graphics for data analysis*. Springer-Verlag New York. ISBN 978–3–319–24277–4. https://ggplot2.tidyverse.org. Accessed Mar 2021
85. Santana MF, Queiroz MV (2015) Transposable elements in fungi: a genomic approach. Sci J Genet Gene Ther 1(1):012–016
86. Coleman JJ, Mylonakis E (2009) Efflux in fungi: La Pièce de Résistance. PLoS Pathog 5(6):e1000486. https://doi.org/10.1371/journal.ppat.1000486
87. Macheleidt J, Mattern DJ, Fischer J, Netzker T, Weber J, Schroeckh V, Valiantem V, Brakhage AA (2016) Regulation and role of fungal secondary metabolites. Annu Rev Genet 50:371–392. https://doi.org/10.1146/annurev-genet-120215-035203
88. Syed K, Yadav JS (2012) P450 monooxygenases (P450ome) of the model white rot fungus *Phanerochaete chrysosporium*. Crit Rev Microbiol 38(4):339–363. https://doi.org/10.3109/1040841X.2012.682050
89. Ichinose H (2013) Cytochrome P450 of wood-rotting basidiomycetes and biotechnological applications. Biotechnol Appl Biochem 60:71–81. https://doi.org/10.1002/bab.1061
90. Qhanya LB, Matowane G, Chen W, Sun Y, Letsimo EM, Parvez M, Yu J-H, Mashele SS, Syed K (2015) Genome-wide annotation and comparative analysis of cytochrome P450 monooxygenases in basidiomycete biotrophic plant pathogens. PLoS ONE 10(11):e0142100. https://doi.org/10.1371/journal.pone.0142100
91. Durairaj P, Hur J-S, Yun H (2016) Versatile biocatalysis of fungal cytochrome P450 monooxygenases. Microb Cell Fact 15:125. https://doi.org/10.1186/s12934-016-0523-6
92. Gonçalves AP, Heller J, Daskalov A, Videra A, Glass NL (2017) Regulated forms of cell death in fungi. Front Microbiol 8:1837. https://doi.org/10.3389/fmicb.2017.01837
93. Schmidt-Dannert C (2014) Biosynthesis of terpenoid natural products in fungi. In: Schrader J., Bohlmann J. (eds) *Biotechnology of isoprenoids. Advances in biochemical engineering/biotechnology*, vol 148. Springer, Cham. DOI: https://doi.org/10.1007/10_2014_283.
94. Quin MB, Flynn CM, Schmidt-Dannert C (2014) Traversing the fungal terpenome. Nat Prod Rep 31(10):1449–1473. https://doi.org/10.1039/c4np00075g
95. Shaw CG III, Roth L (1978) Control of Armillaria root rot in managed coniferous forests. Eur J For Pathol 8:163–174. https://doi.org/10.1111/j.1439-0329.1978.tb01463.x
96. Coetzee MPA, Wingfield BD, Wingfield MJ (2018) Armillaria root-rot pathogens: species boundaries and global distribution. MDPI Pathogens 7:83. https://doi.org/10.3390/pathogens7040083
97. Burdsall HH, Volk TJ (2008) *Armillaria solidipes*, an older name for the fungus called *Armillaria ostoyae*. North American Fungi 3:261–267. https://doi.org/10.2509/naf2008.003.00717
98. Presti LL, Lanver D, Schweizer G, Tanaka S, Liang L, Tollot M, Zuccaro A, Reissmann S, Kahmann R (2015) Fungal effectors and plant susceptibility. Annu Rev Plant Biol 66:513–545. https://doi.org/10.1146/annurev-arplant-043014-114623
99. Kim K, Jeon J, Choi J, Cheong K, Song H, Choi G, Kang S, Lee Y (2016) Kingdom-wide analysis of fungal small secreted proteins (SSPs) reveals their potential role in host association. Front Plant Sci 7:186. https://doi.org/10.3389/fpls.2016.00186
100. Zhao Z, Liu H, Wang C, Xu J-R (2013) Comparative analysis of fungal genomes reveals different plant cell wall degrading capacity in fungi. BMC Genomics 14:274–288. https://doi.org/10.1186/1471-2164-14-274
101. Krijger J-J, Thon MR, Deising HB, Wirsel SGR (2014) Compositions of fungal secretomes indicate a greater impact of phylogenetic history than lifestyle adaptation. BMC Genomics 15:722–739. https://doi.org/10.1186/1471-2164-15-722
102. Varrot A, Basheer SM, Imberty A (2013) Fungal lectins: structure, function and potential applications. Curr Opin Struct Biol 23:678–685. https://doi.org/10.1016/j.sbi.2013.07.007
103. Sahu N, Merényi Z, Bálint B, Kiss B, Sipos G, Owens R, Nagy LG (2020) Hallmarks of basidiomycete soft- and white-rot in wood-decay-omics data of Armillaria. bioRxiv 2020.05.04.075879. https://doi.org/10.1101/2020.05.04.075879.
104. Neuwald AF, Aravind L, Altschul SF (2018) Inferring joint sequence-structural determinants of protein functional specificity. eLIFE 7:e29880. https://doi.org/10.7554/eLife.29880.001.
105. Palma-Guerrero J, Ma X, Torriani SFF, Zala M, Francisco CS, Hartmann FE, Croll D, McDonald BA (2017) Comparative transcriptome analyses in Zymoseptoria tritici reveal significant differences in gene expression among strains during plant infection. Mol Plant Microbe Interact 30:231–244. https://doi.org/10.1094/MPMI-07-16-0146-R
106. Kimura M, Takai T, Takahashi-Ando N, Ahsato S, Fujimura M (2007) Molecular and genetic studies of *Fusarium* trichothecene biosynthesis: pathways, genes, and evolution. Biosci Biotechnol Biochem 71:1–19. https://doi.org/10.1271/bbb.70183
107. Schmidt R, Etalo DW, de Jager V, Gerards S, Zweers H, de Boer W, Garbeva P (2016) Microbial small talk: volatiles in

fungal–bacterial interactions. Front Microbiol 6:1495. https://doi.org/10.3389/fmicb.2015.01495
108. Deveau A, Bonito G, Uehling J, Paoletti M, Becker M, Bindschedler S, Hacquard S, Hervé V, Labbé J, Lastovetsky OA, Mieszkin S, Millet LJ, Vajna B, Junier P, Bonfante P, Krom BP, Olsson S, Dirk van Elsas J, Wick LY (2018) Bacterial–fungal interactions: ecology, mechanisms and challenges. FEMS Microbiol Rev 42:335–352. https://doi.org/10.1093/femsre/fuy008
109. Huang AC, Osbourn A (2019) Plant terpenes that mediate below-ground interactions: prospects for bioengineering terpenoids for plant protection. Pest Manag Sci 75:2368–2377. https://doi.org/10.1002/ps.5410
110. Farh ME, Jeon J (2020) Roles of fungal volatiles from perspective of distinct lifestyles in filamentous fungi. Plant Pathol J 36:193–203. https://doi.org/10.5423/PPJ.RW.02.2020.0025
111. Proctor RH, McCormick SP, Kim H, Cardoza RE, Stanley AM, Lindo L, Kelly A, Brown DW, Lee T, Vaughan MM, Alexander NJ, Busman M, Gutiérrez S (2018) Evolution of structural diversity of trichothecenes, a family of toxins produced by plant pathogenic and entomopathogenic fungi. PLoS Pathog 14(4):e1006946. https://doi.org/10.1371/journal.ppat.1006946
112. Holmes AJ, Tujula NA, Holley M, Contos A, James JM, Rogers P, Gillings MR (2001) Phylogenetic structure of unusual aquatic microbial formations in Nullarbor caves, Australia. Environ Microbiol 3:256–264. https://doi.org/10.1046/j.1462-2920.2001.00187.x
113. Schabereiter-Gurtner C, Saiz-Jimenez C, Piñar G, Lubitz W, Rölleke S (2002) Phylogenetic 16S rRNA analysis reveals the presence of complex and partly unknown bacterial communities in Tito Bustillo cave, Spain, and on its Paleolithic paintings. Environ Microbiol 4:392–400. https://doi.org/10.1046/j.1462-2920.2002.00303.x
114. Zhu H-Z, Zhang ZF, Zhou N, Jiang CY, Wang BJ, Cai L, Liu S-J (2019) Diversity, distribution and co-occurrence patterns of bacterial communities in a karst cave system. Front Microbiol 10:1726. https://doi.org/10.3389/fmicb.2019.01726
115. Sjöberg S, Stairs CW, Allard B, Homa F, Martin T, Sjöberg V, Ettema TJG, Dupraz C. (2020) Microbiomes in a manganese oxide producing ecosystem in the Ytterby mine, Sweden: impact on metal mobility. FEMS Microbiology Ecology. 96. https://doi.org/10.1093/femsec/fiaa169
116. Barriuso J, Márin S, Mellado RP (2010) Effects of the herbicide glyphosate-tolerant maize rhizobacteria communities: a comparison with pre-emergency applied herbicide consisting of a combination of acetochlor and terbuthylazine. Environ Microbiol 12:1021–1030. https://doi.org/10.1111/j.1462-2920.2009.02146.x
117. Bian X, Xiao S, Zhao Y, Xu Y, Yang H, Zhang L (2020) Comparative analysis of rhizosphere soil physiochemical characteristics and microbial communities between rusty and healthy ginseng root. Sci Rep 10:15756. https://doi.org/10.1038/s41598-020-71024-8
118. Nusslein K, Tiedje JM (1999) Soil bacterial community shift correlated with change from forest to pasture vegetation in a tropical soil. Appl Environ Microbiol 65:3622–3626. https://doi.org/10.1128/AEM.65.8.3622-3626.1999
119. Köberl M, Dita M, Martinuz A, Staver C, Berg G (2017) Member of Gammaproteobacteria as indicator species of healthy banana plants on Fusarium wilt-infested fields in Central America. Sci Rep 7:45318. https://doi.org/10.1038/srep45318
120. Byers A-K, Condron L, O'Callaghan M, Waipara N, Black A (2020) Soil microbial community restructuring and functional changes in ancient kauri (*Agathis australis*) forest impacted by the invasive pathogen *Phytophthora agathidicida*. Soil Biol Biochem 150:108016. https://doi.org/10.1016/j.soilbio.2020.108016
121. Przemieniecki SW, Damszel M, Ciesielski S, Kubiak K, Mastalerz J, Sierota Z, Gorczyca A (2021) Bacterial microbiome in *Armillaria ostoyae* rhizomorphs inhabiting the root zone during progressively dying Scots pine. Appl Soil Ecol 164:103929. https://doi.org/10.1016/j.apsoil.2021.103929
122. Saccá ML, Manici LM, Caputo F, Frisullo S (2019) Changes in rhizosphere bacterial communities associated with tree decline: grapevine esca syndrome case study. Can J Microbiol 65:930–943. https://doi.org/10.1139/cjm-2019-0384
123. Liu J, He X, Sun J, Ma Y (2021) A degeneration gradient of poplar trees contributes to the taxonomic, functional, and resistome diversity of bacterial communities in rhizosphere soils. Int J Mol Sci 22:3438. https://doi.org/10.3390/ijms22073438
124. Tong A-Z, Liu W, Liu Q, Xia G-Q, Zhu J-Y (2021) Diversity and composition of the Panax ginseng rhizosphere microbiome in various cultivation modes and ages. BMC Microbiol 21:18. https://doi.org/10.1186/s12866-020-02081-2
125. Balestrini R, Lumini E, Borriello R, Biancotto V (2014) Plant-soil biota interactions. In: E.A. Paul (4th ed.), *Soil microbiology, ecology, and biochemistry*. Cambridge, MA: Academic Press. p. 311–338. eBook ISBN: 9780123914118. https://doi.org/10.1016/C2011-0-05497-2.
126. Horton BW, Glen M, Davidson NJ, Ratkowsky D, Close DC, Wardlaw TJ, Mohammed C (2013) Temperate eucalypt forest decline is linked to altered mycorrhizal communities mediated by soil chemistry. For Ecol Manage 302:329–337. https://doi.org/10.1016/j.foreco.2013.04.006
127. Kipfer T, Egli S, Ghazoul J, Moser B, Wohlgemuth T (2010) Susceptibility of ectomycorrhizal fungi to soil heating. Fungal Biol 114:467–472. https://doi.org/10.1016/j.funbio.2010.03.008
128. Rudawska M, Leski T, Stasinska M (2011) Species and functional diversity of ectomycorrhizal fungal communities on Scots pine (*Pinus sylvestris* L.) trees on three different sites. Annual of Forest Science 68:5–15. https://doi.org/10.1007/s13595-101-0002-x